STRUCTURAL STYLE OF THE SAN FRANCISCO MOUNTAINS, SEVIER FOLD-THRUST BELT, UTAH

A Thesis

presented to the

Faculty of the Graduate School

at the University of Missouri-Columbia

In Partial Fulfillment

of the Requirements for the Degree

Master of Science

---

by

NATHAN GENE REED

Dr. Tandis Bidgoli, Thesis Supervisor

JULY 2022

The undersigned, appointed by the dean of the Graduate School, has examined the thesis entitled

STRUCTURAL STYLE OF THE SAN FRANCISCO MOUNTAINS, SEVIER FOLD-THRUST BELT, UTAH

Presented by Nathan Gene Reed,

A candidate for the degree of Master of Science, and hereby certify that, in their opinion, it is worthy of acceptance.

_____

Assistant Professor Tandis Bidgoli

_____

Associate Professor Francisco Gomez

_____

Assistant Professor Clayton Blodgett

ACKNOWLEDGMENTS

I would like to thank the Department of Geological Sciences for the funding to complete this project. I would also like to thank the StraboSpot team for their funding and software to complete the geologic mapping of this project. I would also like to thank the faculty of the Department of Geological Sciences for my time at Mizzou. I enjoyed all my courses and it was a pleasure to be a part of this department.

I would like to give a special thanks to my advisor, Tandis Bidgoli, for all your support through my graduate education. You are brilliant and I have learned so much from you in the past couple of years not only about geology, but about life. Thank you for being there and supporting me through a very tough time in my life. I am privileged to have a caring advisor such as you. It is much appreciated and I cannot express enough gratitude. I would also like to thank my committee members, Francisco Gomez, and Clayton Blodgett, for their help and feedback on my thesis research.

I would like to thank the all people that helped me with my field work and samples. To my good friends Jordan McMillan, Joshua Jones, and Benjamin Azua, thank you for joining me out in the field. I had a lot of fun and made some awesome memories. To Noah Cadwell, thank you for helping me process my samples. It was a lot of work and having an assistant was super helpful. To Dr. Douglas Walker, thank you for letting me use the Ford Ranger for my field work, she ran like a champ. To Kimberly Moore, thank you for all your help throughout my graduate career and thank you for joining me for that long stretch of field work. You have been a good new friend to me and field work was awesome so long as we don’t get lost. To all the students in the Department of Geological Sciences, it

was nice to have people to bounce ideas off of and go through the graduate school experience together.

I would also like to thank Dr. Wanda Taylor. You sparked my curiosity of structural geology as an undergraduate and you gave me the opportunity to be a part of your research. Thank you for helping me and pushing me to pursue a graduate degree.

I would like to thank my family including my brothers Jonathan Reed and Jeremy Reed, my sister Nadiya Reed, and my stepfather Lorne Crawford for all the love and support. Most importantly I would like to thank my mom, Norma Jean Reed, for always supporting me and standing behind me through all my failures and triumphs in my life. You always had confidence in me and pushed me to succeed. I do not have enough words to express my gratitude to have a mom like you. Sadly you are not here to be able to witness this accomplishment as I know how proud you would be. I love you and miss you so much Mom.

TABLE OF CONTENTS

LIST OF FIGURES

LIST OF TABLES

ABSTRACT

The Sevier fold-thrust belt contains thrust sheets that are overprinted by extensional faults, distorting correlations of geologic structures in the region. The Frisco thrust is exposed within the San Francisco Mountains in west-central Utah. Correlations with the better studied Canyon Range-Willard thrust to the north and the Wah Wah thrust to the south are not well established. The Canyon Range thrust to the north has a forward-breaking sequence, a minimum of 100 km of shortening, and timing is constrained to 145-100 Ma (Pujols et al., 2020). The Willard thrust farther north, has a minimum of 60 km of shortening, and timing is constrained to 125-92 Ma (Yonkee et al., 2019). By comparison, the Wah Wah thrust has a backward-breaking sequence in its footwall, a minimum of 38 km of shortening, and timing that is poorly constrained (Friedrich and Bartley, 2003). This study tests these thrust correlations by examining the geometry, kinematics, and timing of the Frisco thrust through new, detailed (1:24,000 scale) geologic mapping, balanced cross-section construction, and structural analysis techniques. Map data reveal five distinct episodes of faulting. The Frisco thrust and related contractional faults that are east vergent and west dipping. Synchronous strike-slip faults are confined to the hanging wall of the Frisco thrust. Four sets of normal faults cut the thrust: (1) north-south striking low-angle normal faults; (2) high-angle normal faults that are buried, in places, by Cenozoic conglomerates; (3) high-angle normal faults that cut the approximately 31 Ma Horn Silver Andesite; and (4) range-bounding Quaternary faults responsible for tilting of the range to its current orientation. The results suggest that the Frisco thrust correlates with the Wah Wah thrust due to its backward-breaking structural style of thrusting. Direct correlations

are unclear due to lack of timing data. Complete structural and timing data are required to directly correlate the Frisco thrust.

CHAPTER 1

Introduction

The western U.S. Cordillera is host to the many mountain ranges that are a result of multiple orogenic events that have taken place through geologic time. Subduction of the ancient Farallon slab beneath the North American plate began in Late Jurassic time and continued for approximately 100 Ma into the Cenozoic (DeCelles, 2004). During this time, several orogenic fold-thrust belts thickened the crust only to be later overprinted by extension and volcanism beginning in the Early Eocene (Dickinson, 2004). The Sevier fold-thrust belt is a part of this tectonic system and serves as a type-example for geologic studies of retroarc shortening overprinted by extension and volcanism.

The San Francisco Mountains, central western Utah, mark the western edge of the Sevier fold-thrust belt and have experienced a complex geologic history of contraction that is overprinted by extension and volcanic cover. Overprinting of the range makes it difficult to correlate and piece together its geologic history and relations to the surrounding region. The San Francisco Mountains host the Frisco thrust, which placed Precambrian strata atop Paleozoic strata. Along-strike correlations of the Frisco thrust with thrust sheets in the surrounding region have been proposed but are not well established (Miller, 1966; Morris, 1983; Hintze et al., 1984; Lemmon and Morris, 1984; Anders et al., 2012). Additionally, shallow dipping normal faults within the range and the surrounding region create further complications.

Published geologic maps covering the range were created at 1:48,000 scale (Hintze et al., 1984; Lemmon and Morris, 1984), but they contain unclear and unreconciled relationships. Besides this limited mapping and a published paper by East (1965), the San Francisco Mountains are relatively understudied. This study presents the results of new detailed geologic mapping (1:24,000 scale) and geometric and kinematic analyses of the Frisco thrust and overprinting faults in the San Francisco Mountains. The data are used to address the following questions: (1) What is the structural style of deformation? (2) Can a new estimate of total shortening be determined? (3) What is the relative timing of deformation? (4) What thrust sheet does the Frisco thrust correlate to? Several hypotheses also emerge. For example, if the Frisco thrust correlates to the Canyon Range-Willard thrust sheet, a forward-breaking thrust sequence should be observed in the footwall. Alternatively, if the Frisco thrust correlates to the Wah Wah thrust sheet, a backward-breaking thrust sequence should be observed in the footwall. If the Frisco thrust correlates to both structures, additional unmapped structures may be required.

Based on the cross-cutting relationships, five episodes of deformation are observable: Mesozoic shortening, two episodes of prevolcanic Paleocene to Eocene (?) extension, postvolcanic Oligocene to Miocene (?) extension, and Pliocene to Quaternary (?) extension. Separate episodes of faulting imply reorientations in the stress field for the range first during contraction, then up to four reorientations for extensional faults.

This study is important for several reasons. (1) The study provides a better understanding of the evolution of mountain belts and how the crust responds to stress from a convergent plate boundary. (2) It also provides insight into the drivers for the breakup of

mountain belts. (3) It develops a more complete regional scale view of the geologic history of the region. (4) It serves as an analog for other contractional and extensional systems.

This study may also have more broad implications for exploration and development of natural resources. The Sevier fold-thrust belt is host to hydrocarbon resources. This study contributes to a better understanding of the strain distributions that influence hydrocarbon trap development and the burial and exhumation of the source, reservoir, and cap rocks. (2) This study also contributes to a better understanding of extensional faults that overprint thrust systems, which can breach hydrocarbon traps and act as a conduit for fluid flow and mineralization and development of critical mineral resources.

CHAPTER 2

Background

Regional Geologic Setting

Triassic to Eocene back-arc shortening in the western North American Cordillera begins with the subduction of the Farallon plate. Eastward convergence of the Farallon plate beneath the North American plate resulted in approximately 335 kilometers of crustal shortening in the retroarc region (DeCelles and Coogan, 2006). This shortening was concentrated in three widely recognized thrust belts in the western Cordillera: the Luning-Fencemaker thrust belt, the Central Nevada thrust belt, and the Sevier thrust belt (Figure 1). The Sevier fold-thrust belt, which extends from Mexico to Canada more than 6000 kilometers (DeCelles, 2004), is the largest fold-thrust belt of the three and is characterized by thin-skinned deformation, forming several distinct thrust sheets in the process of shortening (Allmendinger and Jordan, 1981). The thrust sheets (Figure 1) that make up the Sevier fold-thrust belt have differing shortening magnitudes and timing (Mitra and Sussman, 1997; Friedrich and Bartley, 2003; Yonkee et al., 2019; Pujols et al., 2020). A regional reconstruction of the Sevier fold-thrust belt suggests approximately 220 kilometers of shortening in central Utah (DeCelles and Coogan, 2006). Shortening in this region initiates in the Late Jurassic and continues into the Late Cretaceous, when it comes to an end (DeCelles and Coogan, 2006). As the subducting Farallon plate shallowed in the Late Cretaceous, arc volcanism shifts position (Humphreys, 2009; Canada et al., 2019).

In the Early Cenozoic, the shallow Farallon plate transmits stresses eastward into the North American interior initiating the Laramide orogeny (Colgan and Henry, 2009). At approximately 50-43 Ma, removal of the Farallon slab allowed hot asthenosphere to come into contact with continental crust causing a large ignimbrite flareup (Dickinson, 2006; Canada et al., 2019). Migration of volcanism, starting in the north near Idaho and moving south toward southern Nevada and Utah, is triggered by the roll-back of the slab (Dickinson, 2006). This volcanism may have weakened the crust as evidenced by the development of metamorphic core complexes and extensional deformation in the Basin and Range Province (Dickinson, 2006). These extensional faults overprinted pre-existing shortening structures. The overprinting of several generations of extensional faults makes it difficult to correlate thrust sheets in the area (Friedrich and Bartley, 2003). Post-volcanic extension continued in the Miocene, as the youngest of the metamorphic core complexes were being exhumed in the eastern Basin and Range (Dickinson, 2006).

The Frisco Thrust

The Frisco thrust, exposed in the San Francisco Mountains in central-western Utah, marks the western edge of the Sevier fold-thrust front (Figure 2). Along-strike correlations and evolution of the Frisco thrust are not well established (Anders et al., 2012). Several thrust correlations have been proposed but are not reconciled. Original thrust correlations were done based on geologic mapping and stratigraphic relations (Morris, 1983; Hintze et al., 1984; Lemmon and Morris, 1984), but as the outcrops are not continuous between adjacent mountain ranges due to extensional structures, these interpretations are uncertain. The Frisco thrust placed Precambrian rocks over Cambrian and Ordovician rocks (Hintze et al., 1984). There is no data on the timing or thermal history of exhumation of the Frisco

thrust. The Frisco thrust also does not have an associated magnitude of shortening. It has been assumed that the Frisco thrust is part of the Wah Wah thrust sheet since the rocks involved are similar, suggesting they are part of the same thrust sheet (Miller, 1966; Morris, 1983), but with little to no evidence to support this. Furthermore, Morris (1983) also suggested that the Frisco thrust could be correlated to the Beaver Lake Mountains thrust to the southeast, but this correlation is also uncertain.

Correlations of the Frisco thrust could tie both the better studied Canyon Range-Willard thrust sheet to the north and the Wah Wah thrust sheet to the south. However, it is unclear how the continuous thrust belt developed. The Canyon Range-Willard thrust and the Wah Wah thrust have different structural styles, amounts of shortening, and timing (Mitra and Sussman, 1997; Friedrich and Bartley, 2003; Yonkee et al., 2019; Pujols et al., 2020). The Frisco thrust lies between an unexplained strain gradient separating the two thrust sheets. If they correlate, some undocumented structures may be between the different thrust sheets.

To the north of the Frisco thrust, the Canyon Range-Willard thrust sheet accommodates 100 kilometers of shortening along the Canyon Range portion of the thrust sheet (Mitra and Sussman, 1997; DeCelles and Coogan, 2006) and 60 kilometers of shortening along the Willard section, farther north (Yonkee et al., 2019). Magnitudes of shortening for the Canyon Range thrust were derived from balanced cross-sections. The Canyon Range thrusts placed Precambrian and Cambrian rocks over Devonian rocks and has been interpreted as a forward-breaking sequence in its footwall (Mitra and Sussman, 1997) (Figure 3). Apatite fission-track ages and modeling suggest the onset of exhumation of the Canyon Range thrust sheet at 146 Ma (Ketcham et al., 1996; Stockli et al., 2001).

Detrital zircon U-Pb geochronology and (U-Th)/He thermochronology were used to constrain the timing of the Canyon Range thrust to 140-101 Ma (Pujols et al., 2020). Age data are integrated into cross-section data to interpret exhumation rate of the thrust sheet. The Willard thrust in the Monte Cristo Range placed Precambrian and Cambrian rocks on Upper Paleozoic and Cretaceous rocks. White mica $^{40}Ar/^{39}Ar$ and fission-track ages indicate thrusting in northern Utah and southeastern Idaho at 140-143 Ma (Yonkee et al., 1989; Burtner and Nigrini, 1994; Yonkee et al., 1997). Zircon (U-Th)/He and fission track thermochronometry data from Yonkee et al. (2019) constrain the amount of shortening as well as the timing of exhumation for the Willard thrust to 125-92 Ma (Yonkee et al., 2019).

In contrast, the Wah Wah thrust, to the south of the Frisco thrust, has a minimum shortening of 38 km (Friedrich and Bartley, 2003). This magnitude is derived from multiple balanced cross-sections taken from geologic map data throughout the Wah Wah Mountains. The hanging wall of the Wah Wah thrust contains similar Precambrian rocks as the Frisco thrust that have been placed over younger Mississippian and Pennsylvanian rocks. Contractional deformation in the Wah Wah Mountains occurred in three stages, revealing a backward-breaking duplex in its footwall (Friedrich and Bartley, 2003) (Figure 3). In the first stage, the Wah Wah thrust breaks from a western detachment, placing Cambrian over Devonian-Silurian rock. In the second stage, the frontal thrust is abandoned and a new thrust breaks from the back creating a hinterland dipping duplex. In the third stage, the frontal thrust is abandoned again and an imbricate splay is formed in the thrust front (Friedrich and Bartley, 2003). Although the geometries of the Wah Wah thrust have been well documented, thrust timing is not well constrained. No age data indicating the exhumation history of the Wah Wah thrust is published.

Problems with Existing Geologic Maps

Published geologic maps within the study area are limited and include questionable map relationships. The finest scale published maps are 1:48,000 geologic maps separated into three 7.5-minute quadrangles: (1) Geologic Map of the Milford Quadrangle and East Half of the Frisco Quadrangle, Beaver County, Utah quadrangles; (2) Geologic Map of the Frisco Peak Quadrangle, Millard and Beaver Counties, Utah; (3) Geologic Map of the Beaver Lake Mountains Quadrangle, Millard and Beaver Counties, Utah (Best et al., 1989; Hintze et al., 1984; Lemmon and Morris, 1984).

At the southern end of the range, mapped by Hintze et al. (1984), there are thrusts mapped in Ordovician units that have clear younger on older relationships according to the mapped stratigraphic units (Figure 4). The Fillmore Formation and House Limestone (Ohf) should lie conformably above the Notch Peak Formation (OCn). This would make the interpretation of a thrust fault incorrect as this is more reasonably to be a normal fault or stratigraphic contact. Similarly, the Notch Peak Formation (OCn) is interpreted as thrust above of the Big Horse Limestone (Cob); however, the Notch Peak Formation (OCn) is stratigraphically younger than the Big Horse Limestone (Cob). These problems persist in the central and north end of the range, mapped by Lemmon and Morris (1984), where the Precambrian Inkom Formation (Zi) is thrust above of the Caddy Canyon Quartzite (Zcc), which it stratigraphically overlies (Figure 4). Farther north, units including the Caddy Canyon Quartzite (Zcc), Inkom Formation (Zi), and Mutual Formation (Zm) are mapped as being thrust on top of the stratigraphically lower Blackrock Canyon Limestone (Zbc).

Normal faults also illustrate conflicting cross-cutting relationships with Cenozoic units, including the Eocene to Oligocene Horn Silver Andesite (Ths) and the Granodiorite

of Cactus Stock (Tgd). Some normal faults are mapped as being buried by these units while others cross-cut them. In the central part of the range, some normal faults are mapped as being buried by the Conglomerate of High Rock Pass (Thr) while others juxtapose it against Precambrian units. While these relationships could be indicative of multiple generations of normal faults, it is difficult to determine from the published maps. Determining the relationships of the faults in the Cenozoic units are important to provide age constraints on timing of extensional overprint.

Stratigraphy

The stratigraphy of the San Francisco Mountains and surrounding region is well defined (East, 1965; Welsh, 1972; Lemmon et al., 1973; Lemmon and Morris, 1984, Hintze et al., 1984, Best et al., 1989; Hintze and Davis, 2002). The established stratigraphy was used for geologic mapping and determining structural relationships. The San Francisco Mountains expose Paleozoic units that are overthrusted by Precambrian strata. These units are unconformably overlain by Paleogene conglomerates of unknown age and volcanic rocks of known age (Figure 4; Plates 1 and 2). Quaternary alluvial deposits fill active stream channels and surround the range in lower elevations (Plate 1). New rock descriptions from new 1:24,000 scale geologic mapping is provided on Plate 1.

Precambrian Stratigraphy

Precambrian strata make up the hanging wall of the Frisco thrust. The upper plate of the Frisco thrust is well exposed throughout the range (Plate 1). Previous works have grouped the Precambrian strata as part of the Cambrian Prospect Mountain Quartzite (Cpm) (East, 1965). While the Cambrian Prospect Mountain Quartzite (Cpm) is the upper

most unit of the Frisco thrust sheet, other older Precambrian strata lie beneath. Later 1:48,000 scale geologic maps recognized and distinguished several older units beneath the Prospect Mountain Quartzite (Cpm), including the Mutual Formation (Zm), the Inkom Formation (Zi) and the Caddy Canyon Quartzite (Zcc) (Hintze et al., 1984; Lemmon and Morris, 1984). The exposed strata consist mainly of shallow marine quartzites with beds of argillite and some limestones (Figure 4; Plate 1). There is an overall coarsening upward trend to these quartzites throughout the units.

Paleozoic Stratigraphy

Paleozoic strata are overthrusted by Precambrian units throughout the range (Plate 1). Exposures consist mainly of Cambrian and Ordovician carbonates with some shale. The upper most strata in the Paleozoic section are the Ordovician Watson Ranch Quartzite (Owr), which is equivalent to the Eureka Quartzite found throughout the Great Basin. These rocks were formed in shallow water marine shelf environments.

Unconformity

Precambrian and Paleozoic rocks in the range are unconformably overlain by Paleogene conglomerates and Eocene to Oligocene volcanic units (Figure 4; Plate 1). The unconformity is important for determining timing of deformation and deposition of Cenozoic units. Where measured, the units have a relatively gentle W-NW dip of ~5°-15° (Plate 1). The unconformity is angular and has a dip of ~20°-35° dipping in various directions throughout the map area (Plate 1).

Cenozoic Stratigraphy

There are two distinct Paleogene conglomerates that are found in the area. The first is a boulder conglomerate that consist of mainly local limestones (~99%). The second is a pebble to cobble conglomerate that contains a majority of local quartzites (~80%). These conglomerates are mainly found in the central and northern part of the range and, in places, unconformably overly units of the Frisco thrust sheet (Plate 1). Ages are not known but there are several locations within the map where these two units are in fault juxtaposition (Plate 1). Neither of the conglomerates contain volcanic clasts and the Horn Silver Andesite (Ths) overlies the conglomerates. Based on these relations, the conglomerates are thought to be older than the volcanic units in the range.

There are two separate volcanic units exposed in the range. The older of the two is the Horn Silver Andesite (Ths) that is found throughout the map area (Plate 1). This rock has K/Ar isotopic ages of 30.8 Ma ± 0.6 Ma for plagioclase and 34.1 Ma ± 0.8 Ma for hornblende (Lemmon et al., 1973). This andesite contains porphyritic flow rocks and some ash-flow tuffs. The younger Granodiorite of Cactus Stock (Tgd) is found in the southern part of the range where it intrudes Paleozoic units (Plate 1). Skarns can be found in adjacent carbonate rocks. This unit has a K/Ar isotopic age of 28.0 Ma ± 0.7 Ma for biotite (Lemmon et al., 1973).

Quaternary alluvial fill occupies active drainages and surrounds the mountains at lower elevations than the bedrock (Plate 1). Alluvium was mapped using NAIP imagery.

Quartzite Breccia

One important unit to note is a breccia that lies within the central part of the range (Plate 1). The breccia was described by East (1965) and recognized on maps by Hintze et al. (1984) and Hintze and Davis (2002). It is only found in the central part of the range and occurs as large mounds (five to thirty m in diameter) of breccia, made up exclusively of quartzite. Different mounded exposures contain different quartzite breccias from the Precambrian strata. The origin and timing of these rocks are unknown, but the unit seems to lie unconformably above of Precambrian quartzites. The rocks may be a shear zone tied with tectonic activity of the San Francisco Mountains; however, mapping in this portion of range was challenging (East, 1965).

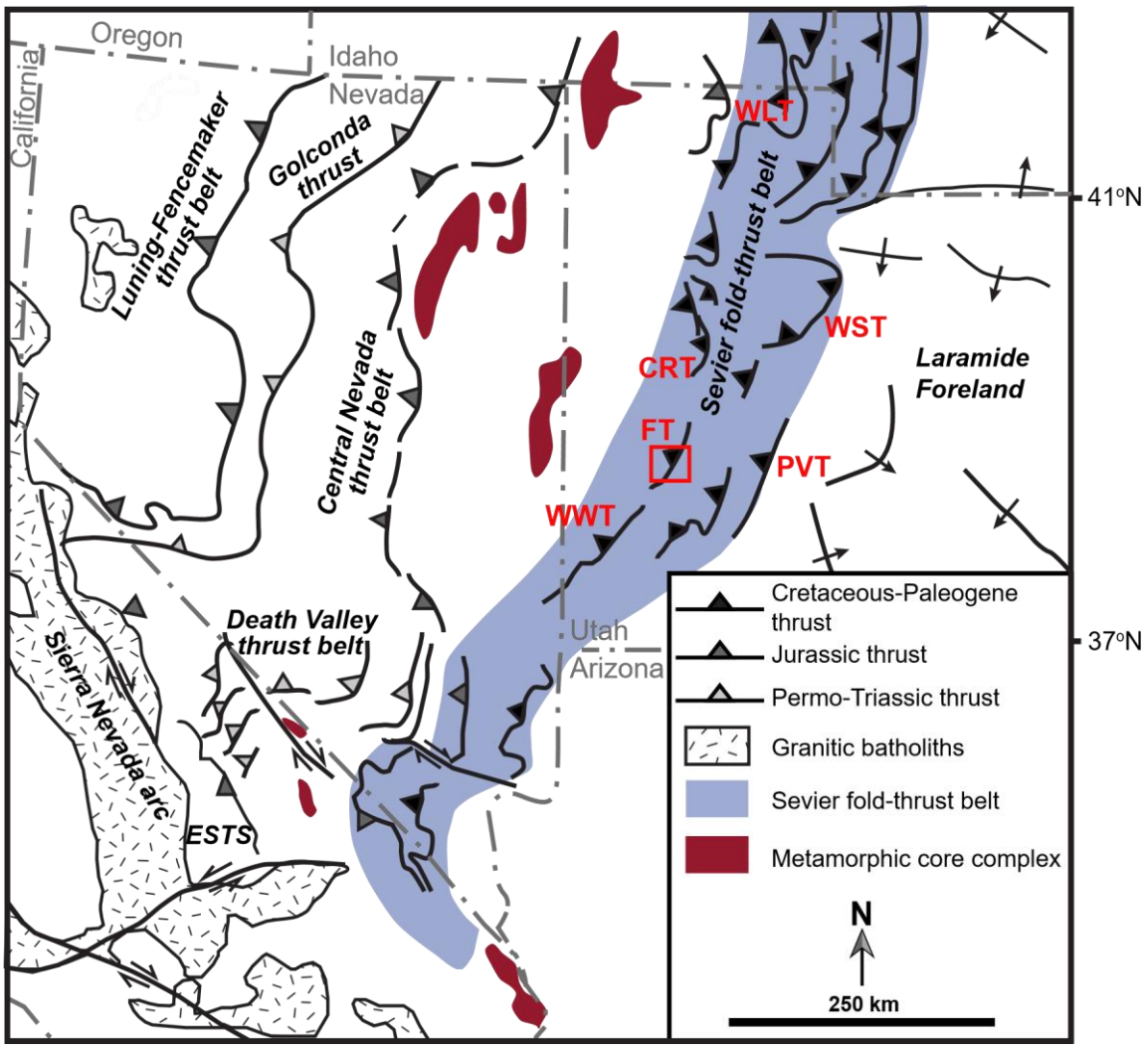

Figure 1. Simplified tectonic map of the North American Cordillera showing the major deformation zone of the Sevier fold-thrust belt and the study area (red box). ESTS- East Sierra thrust system; WWT- Wah Wah thrust; FT- Frisco thrust; CRT- Canyon Range thrust; PVT- Pavant thrust; WST- Wasatch thrust; WLT- Willard thrust. Modified from Wyld and Wright (2001), DeCelles (2004), and Dunne and Walker (2004).

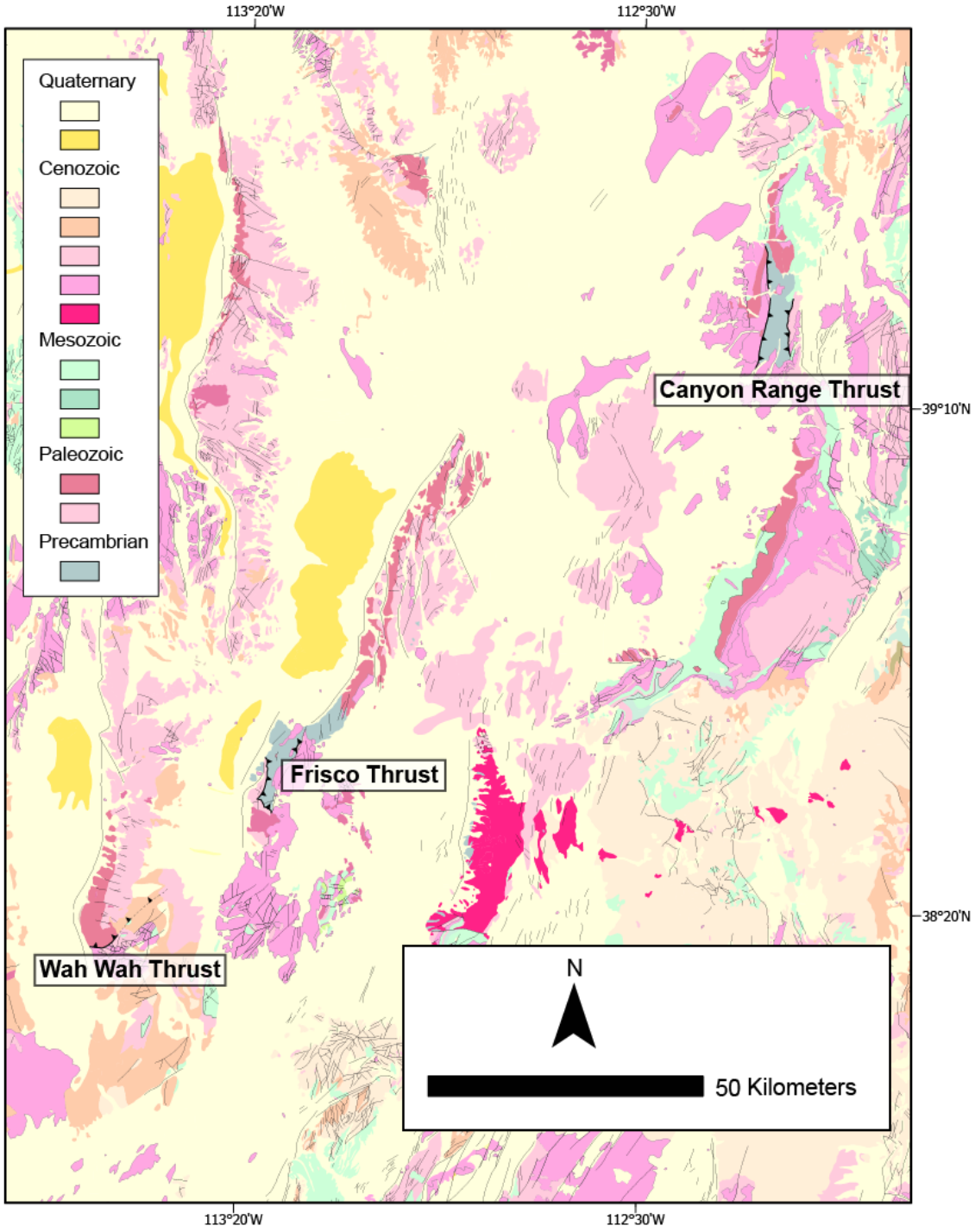

Figure 2. Simplified geologic map of central western Utah showing the location of the Wah Wah thrust, Frisco thrust, and the Canyon Range thrust. Modified from U.S. Geological Survey (2007).

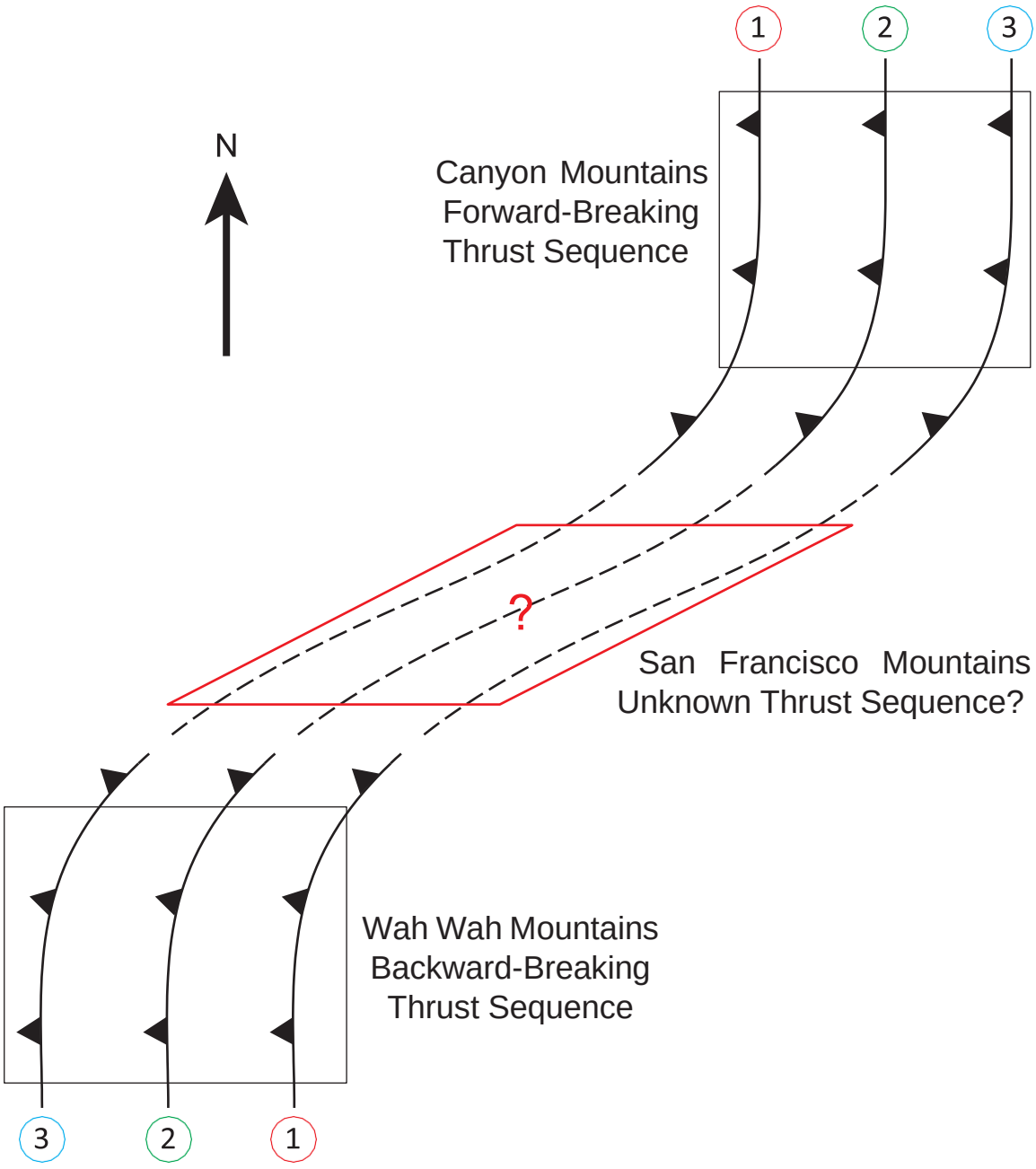

Figure 3. Schematic diagram of thrusts in map view. The numbers 1, 2, and 3 represent the thrust sequence for the Wah Wah thrust and the Canyon Range thrust with the uncertain study area in between where the San Francisco Mountains are located. Thrust sequence is reversed from the Wah Wah Mountains to the Canyon Mountains.

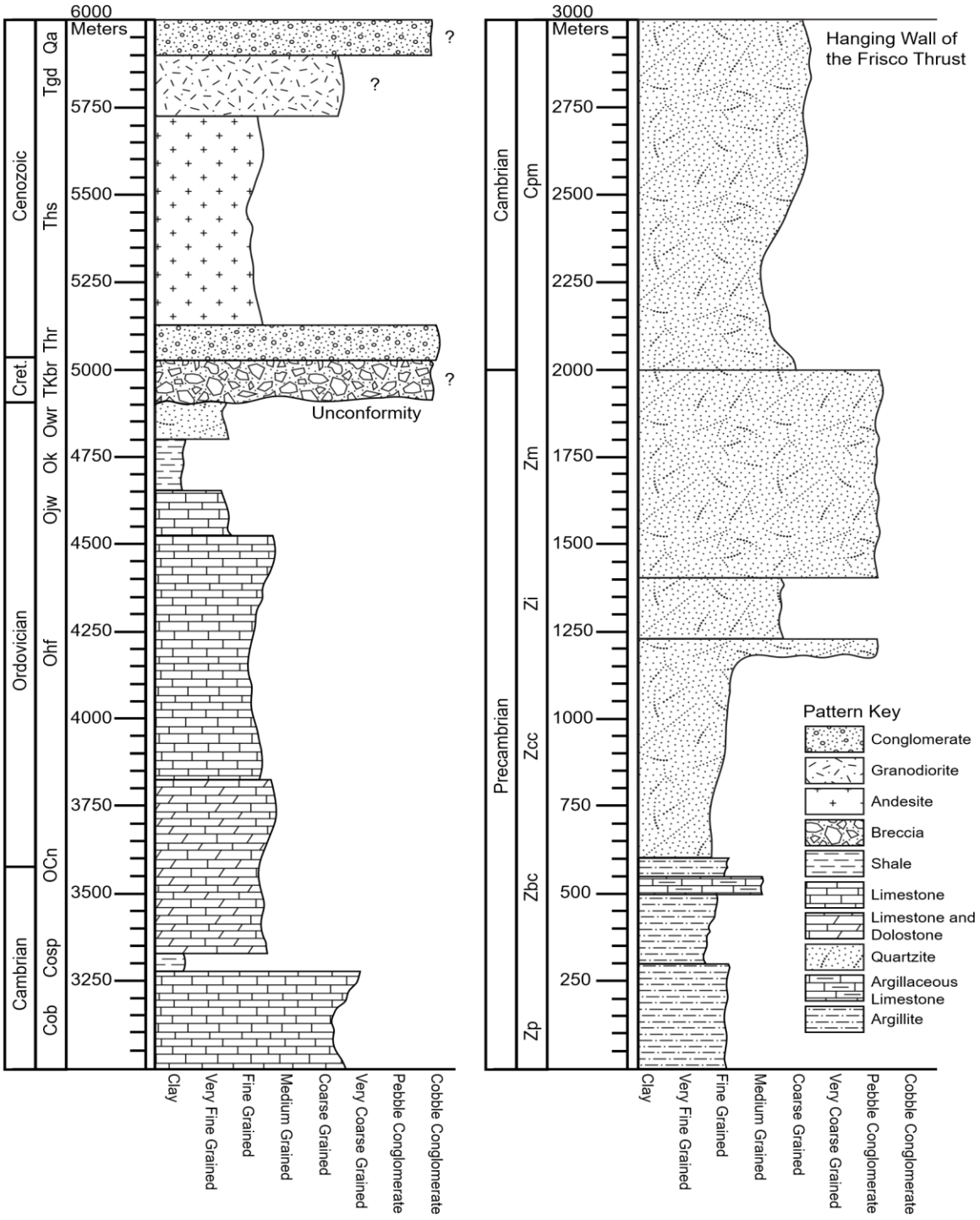

Figure 4. Stratigraphy of the San Francisco Mountains, Utah. Stratigraphic thickness is based on exposed thickness in the study area and published data from Hintze and Davis (2003). Standard lithologic patterns are used. Two columns separate the hanging wall and the footwall of the Frisco thrust.

CHAPTER 3

Methods

Geologic Mapping

Standard geologic techniques were used to map ~60 km^2 in the San Francisco Mountains, Utah at 1:24,000 scale. The map area covers portions of the Milford NW Quadrangle, Frisco Quadrangle, Frisco Peak Quadrangle, High Rock Quadrangle, Iron Mine Pass Quadrangle, and the Brown Knoll Quadrangle, USGS 7.5-minute quadrangles. NAIP (National Agriculture Imagery Program) aerial images of the same quadrangles were used to map the Quaternary surficial geology and to aid in bedrock mapping and interpretations. Portions of the Geologic Map of the Frisco Peak Quadrangle, Millard and Beaver Counties, Utah (Hintze et al., 1984) and the Geologic Map of the Beaver Lake Mountains Quadrangle (Lemmon and Morris, 1984) were incorporated to fill any missing portions of the new map data (Plates 1 and 2). Geologic map data were collected digitally using StraboSpot 2 software (version 1.0.1) on an iPad (6^{th} generation). Collected data were then transferred into ArcGIS Pro (version 2.7.0). Final geologic map data were input and edited in Adobe Illustrator (version 25.4.1) (Plates 1 and 2).

Structural Analysis

Four structural analysis techniques were used to analyze the geologic map data. (1) Fault orientations and geometries that could not be collected in the field were calculated using a 3-point strike-dip calculator in Microsoft Excel (version 2201 build

16.0.14827.20180). Strikes and dips were determined by entering three points on a plane using elevations from the USGS topographic base maps and locations using UTM coordinates in ArcGIS Pro (version 2.7.0). (2) Stereoplots of faults and folds were created using Stereonet (version 11.3.6) (Allmendinger et al., 2013; Cardozo et al., 2013; Allmendinger, 2021) (Figures 5 and 6). Stereoplots allow structural data to be differentiated by fault type and orientation, and by fold hinge attitudes. Fault attitudes were separated by fault type, and faults with normal separations were grouped by similarities in strike (Figure 5). Folds are represented by their π-axes (Figure 6). (3) Stereoplots of kinematic data were created using FaultKin (version 8.1.2) (Marrett and Allmendinger, 1990; Allmendinger et al., 2012; Allmendinger, 2019) (Figure 7). FaultKin analyzes fault geometric and kinematic data and provides P (shortening) and T (extension) axes as well as principle stress axes. Stereoplots were separated by kinematic indicators measured from strike-slip faults and faults with normal separations (Figure 7). (4) Balanced cross-sections were constructed using standard line-length balancing techniques (Dahlstrom, 1969; Gibbs, 1983; Rowan and Kligfield, 1989; Groshong, 1994). A fence-diagram was constructed to link the cross-sections and perform an area balance (Figure 10). The cross-sections provide information on the subsurface geology, kinematics of faults, and 2D and 3D strain distributions.

CHAPTER 4

Results

Fault Descriptions

A total of 182 fault segments were mapped in the San Francisco Mountains, Utah (Plate 1). Faults in the field were identified by offset features, juxtaposed stratigraphic units, fault gouge, fault breccia, and fault surfaces. The mapped faults and their cross-cutting relationships reveal several episodes of contractional and extensional deformation. Thrusting occurred in the Cretaceous (?), while extension occurred during at least three time intervals: (1) a prevolcanic Paleocene to Eocene (?), (2) postvolcanic Oligocene to Miocene (?), and (3) Pliocene to Quaternary (?) episodes. The extensional episodes are defined by their cross-cutting relationship with the Paleocene (?) Conglomerate of High Rock Pass, Oligocene Horn Silver Andesite, their geometry, and their differences in strike (Figure 5). Fault sets are listed in relative order, from oldest to youngest.

Thrust Faults

Thirteen north-south striking thrust fault segments were mapped in the area (Figure 5). The faults can be divided into two groups based on their hanging wall and footwall associations. The first group consists of thrust faults exposed in the southern and central part of the range (Plate 1). These faults characterize the Frisco thrust. The faults placed Precambrian Caddy Canyon Quartzite (Zcc) on Ordovician to Cambrian sedimentary rocks (Plate 1). These faults strike north-south and dip to the west and with dips ranging from

4°- 26° with one outlier of 35° dip. The faults are planar with an apparent reverse separation. The faults get buried by both the Conglomerate of High Rock Pass (Thr) and the Horn Silver Andesite (Ths). The second group consists of thrust faults that display repeating section of Precambrian strata in the hanging wall of the Frisco thrust exposed in the central part of the range (Plate 1). These faults dip to the west and have dips ranging from 7°- 16°. The faults are planar with an apparent reverse sense of displacement. Minimum displacement for these faults is 2.1 km. Fault breccia can be found at some of the contacts but most of the contacts are buried and are determined by their placement over younger strata.

Strike-Slip Faults

Thirty-six strike-slip fault segments were measured in the map area (Figure 5). The strike-slip faults appear to be confined to the hanging wall of the Frisco thrust in the northern part of the range and are mostly contained within the Caddy Canyon Quartzite (Zcc) and the Blackrock Canyon Limestone (Zbc) (Plate 1). There are two sets of faults, one set strikes north-south and the second set strikes northeast-southwest. Dips for the faults are east and west, ranging from 54°- 90°, with the majority dipping >70°. The faults are planar and have both apparent left-lateral and right-lateral stratigraphic separations. The faults have minor (<10 m) offset; however, a few have larger offset of up to 150 m. The faults crop out as mounds with fault polish and planar features. The kinematic indicators have rakes ranging from 4°- 33°, with the majority of rakes <15°, indicating mainly strike-slip motion.

Low-Angle Normal Faults

Fourteen low-angle normal fault segments were recorded in the mapping area (Figure 5). The faults are found in both the southern and northern ends of the range (Plate 1). In the southern end of the range, the faults strike north-south and dip to the east, with dips measuring from 4°- 22°. The faults are planar and have apparent normal separation. They excise the full thickness of the Steamboat Pass Shale (Cosp) that should be found stratigraphically above of the Big Horse Limestone (Cob). A large gouge zone is present at the contact between the Big Horse Formation (Cob) and the Notch Peak Formation (OCn) where the Steamboat Pass Shale (Cosp) should be present. This fault has a minimum stratigraphic separation of 360 m. Also in the south end of the range, the full thickness of the Fillmore Formation and House Limestone (Ohf) member of the Pogonip Group has been removed. This fault has a minimum stratigraphic separation of 3300 m. In the north end of the range, the faults strike northeast-southwest and dip to the west with dips measuring from 15°- 23°. These faults are planar and have apparent normal separations. The upper member of the Blackrock Canyon Limestone (Zbc) is excised and the contacts are poorly exposed or buried. The minimum stratigraphic separation across these faults is 1000 m. The faults are believed to be Paleocene or older as they do not cut any of the Cenozoic units. The low-angle normal faults in the map are cross-cut by several fault sets, suggesting they are older than the other extensional structures in the map area.

Northwest-Southeast Striking Normal Faults

Forty-two northwest-southeast fault segments were recorded in the mapping area (Figure 5). These faults are mainly confined to the central part of the range and occur

between larger northeast-southwest striking faults (Plate 1). Most of the faults cut through the Precambrian hanging wall units of the Frisco thrust but are exposed in some of the Paleozoic footwall units of the Frisco thrust. These faults juxtapose units in the hanging wall of the Frisco thrust at the surface. Their relative timing is inferred to be synchronous with the northeast-southwest striking faults as these faults cannot be traced across these structures. These faults do not cut any of the Cenozoic units. The dip directions vary but most of the faults are dipping north or south, with dips ranging from 41°- 86°. The faults that dip to the east and west have dips that range from 41°- 89°. The majority of the faults are planar but some of them are nonplanar, mainly the faults that follow down washes or topographic lows. Minimum stratigraphic offsets for these faults are 40 m. The apparent separation across the faults is normal. Kinematic indicators were taken from exposed fault planes and slickenlines. The rakes on these planes range from 61°- 86°, indicating dip-slip and oblique-slip motion.

Northeast-Southwest Striking Normal Faults

Thirty-two northeast-southwest fault segments were mapped in the area (Figure 5). The faults can be found throughout the range and occur as longer fault strands (Plate 1). The faults cut through both the Precambrian hanging wall and Paleozoic footwall units of the Frisco thrust. The faults juxtapose units in the hanging wall of the Frisco thrust next to the footwall units in the south end of the range. In the central and northern part of the range, hanging wall units are juxtaposed across these faults. The faults are buried, in places, by the Paleocene (?) Conglomerate of High Rock Pass (Thr) and the Oligocene Horn Silver Andesite (Ths). The cross-cutting relationships suggest these faults are synchronous with the northwest-southeast striking and the north-south striking faults confined between them,

but older than the youngest set of north-south striking faults. The faults are both planar and nonplanar as some of the faults have bends along-strike. Faults dip both east and west, 31°-88°. Minimum stratigraphic separations for these faults are apparent normal and vary from 300 m to 800 m. Fault surface exposures were limited but where kinematic indicators could be measured, they have rakes of 47°- 72°. This would suggest dip-slip and oblique-slip motion along these faults.

North-South Striking Normal Faults

Forty-five north-south striking fault segments were recorded in the mapping area (Figure 5). There are three sets of north-south striking faults that have different relative ages. The first set are located in the southern and northern parts of the range (Plate 1). In the southern part of the range, the faults cut the low-angle normal faults that in turn cut Paleozoic units and the Frisco thrust. The faults dip east and west and range in dip from 50°- 88°. Apparent separation is normal on these planar faults. Kinematic indicators have rakes of 78°- 83° and suggest dip-slip displacements. There is a minimum of 60 m of stratigraphic separation across these faults. In the northern part of the map area, the faults cut hanging wall units of the Frisco thrust and juxtapose the Precambrian Caddy Canyon Quartzite (Zcc) against the Blackrock Canyon Limestone (Zbc). The faults dip west and have dips ranging from 40°- 88°. The faults are planar with stratigraphic separation of up to 900 m. The faults are not well exposed at the surface and have apparent normal separation.

The second set of north-south striking faults is located in the central part of the range confined between the northeast-southwest striking faults (Plate 1). The faults cut through Precambrian units of the hanging wall of the Frisco thrust and also cut the Frisco

thrust. The faults dip both east and west, with dips ranging from 48°- 89°. Apparent separations are normal. Most of the faults are planar but there are some nonplanar faults mapped. Kinematic indicators of exposed fault planes have rakes of 61°- 86° suggesting dip-slip and oblique-slip displacements. Minimum stratigraphic separations are as low as 40 m. The timing of these faults is likely synchronous with the northeast-southwest striking faults since they cannot be traced across them.

The third set of north-south striking faults is located in the southern part of the range (Plate 1). The faults cut the Oligocene Horn Silver Andesite (Ths) and juxtapose it with the Caddy Canyon Quartzite (Zcc) and the Conglomerate of High Rock Pass (Thr), in places. The faults dip east with dips ranging from 61°- 84°. Exposed fault surfaces have groove and mullion measurements with rakes of 87°, suggesting dip-slip motion. Other exposures of these faults are poor, but apparent separations are normal. Minimum stratigraphic offset is not known since the Horn Silver andesite can vary significantly in thickness. The relative age of the faults seems to be the youngest of the north-south striking faults in the range.

Fold Descriptions

A total of fifteen folds were mapped in the San Francisco Mountains, Utah (Plate 1). Folds in the field were identified by the changes in the dip of stratigraphic units. Folds occur in both the hanging wall and the footwall of the Frisco thrust. Folds are recognized in different areas of the map and in cross-section (Plates 1 and 2). Folds are represented by their π-axes in Figure 6.

Three folds are documented in the southern portion of the map. All of the folds are antiforms in Paleozoic footwall units of the Frisco thrust (Plate 1). The folds are cut by north-south striking faults. In their current orientation, two of the folds are northeast-

southwest trending and one of the folds is trending east-west. All three of the folds are non-plunging (1.7°- 3.2°), upright folds (79°- 87°), open folds. Projections of these folds in the subsurface were required to balance and restore cross-sections (Plate 2).

Eight folds are documented in the central part of the range. The folds occur in Precambrian quartzites that make up the footwall of the Frisco thrust (Plate 1). There are both synform and antiform structures present. The folds are cut by the northwest-southeast striking faults, the northeast-southwest striking faults, and the north-south striking faults. The map-scale folds have wavelengths ranging from 900 m to 1070 m while the smaller scale folds have wavelengths ranging from 60 m to 300 m (Plates 1 and 2). Most of the folds are northeast-southwest trending with a few of the folds trending east-west. All of the folds are non-plunging (0.4°- 5.6°), upright (79°- 89°), open folds. Projections of these folds in the subsurface were required to balance and restore cross-sections (Plate 2).

Four folds were recorded in the northern part of the range. The folds are in different members of the Precambrian Blackrock Canyon Limestone (Zbc). There are both synform and antiform structures present. No faults cut the folds but they are found just beneath the northeast-southwest low-angle normal fault. These folds consist of several smaller folds with wavelengths of a few meters. There wavelength is too tight to capture at 1:24,000 map scale. The folds are northeast-southwest trending, non-plunging to moderately plunging (3.2°- 38°), upright to moderately inclined (79°- 87°), tight folds.

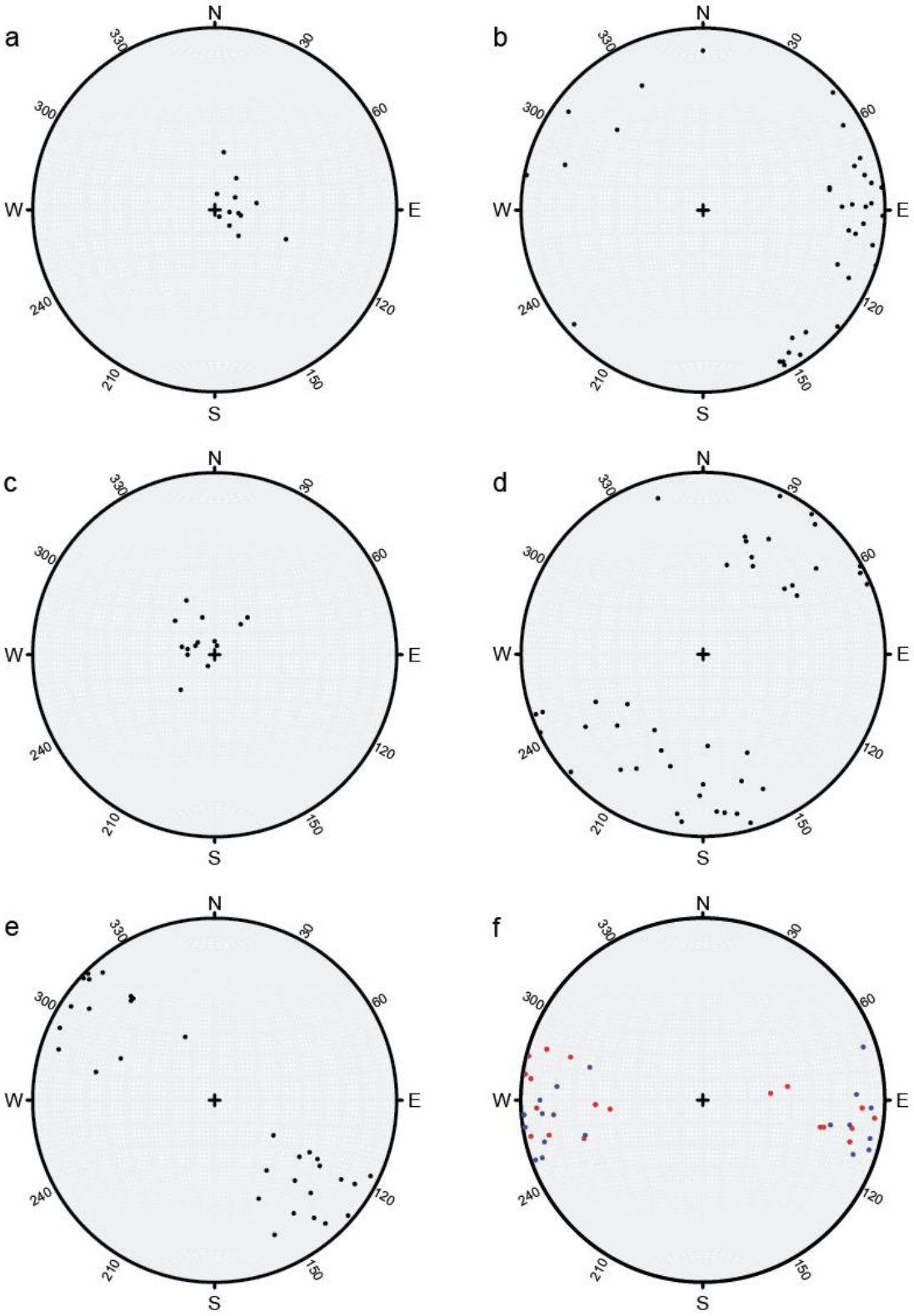
a
b
c
d
e
f
N
S
E
W
30
60
120
150
210
240
300
330

Figure 5. Stereoplots of faults. Lower hemisphere equal-area projection of poles to (a) thrust faults, (b) strike-slip faults, (c) low-angle normal faults, (d) northwest-southeast striking normal faults, (e) northeast-southwest striking normal faults, and (f) north-south striking normal faults. North-south normal faults are distinguished by color (blue- faults located in the south end of the range, red- faults located in the center of the range). Stereoplots were made using Stereonet v. 11.3.6 (Allmendinger, 2021). Structural data used to create Stereoplots are listed in Tables 1-7, Appendix I.

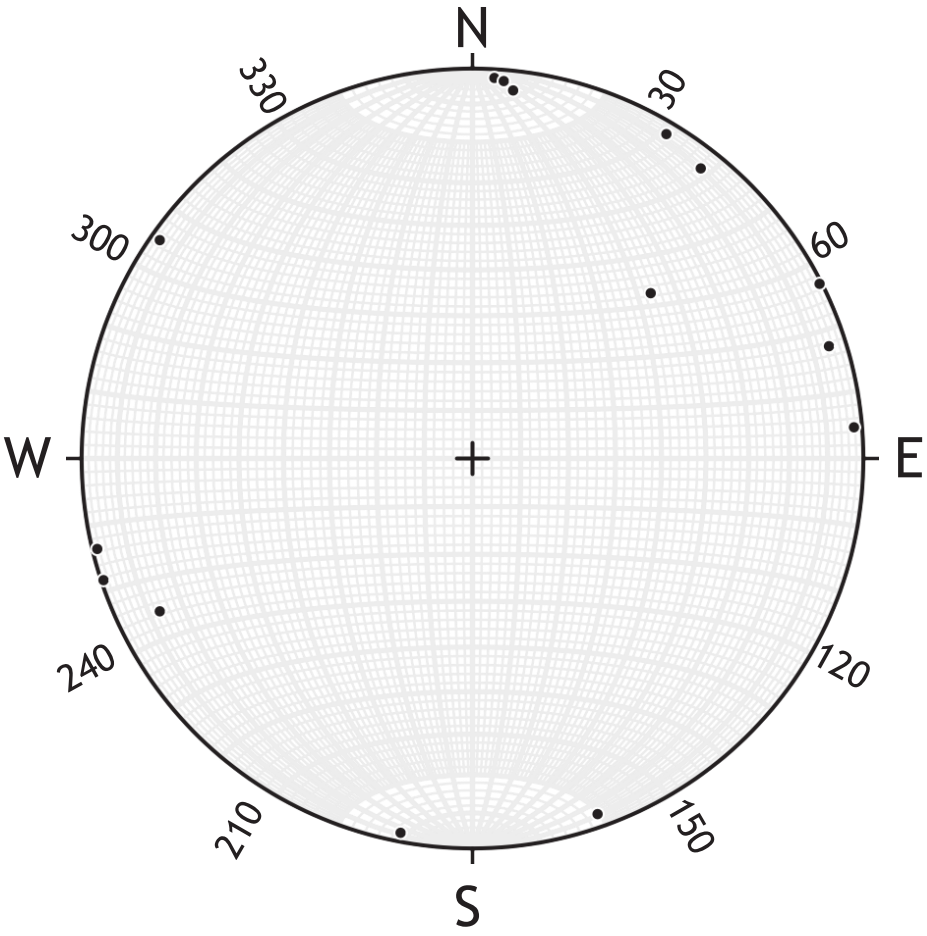

Figure 6. Stereoplots of folds. Lower hemisphere, equal-area projection of π-axes. Stereoplots were made using Stereonet v. 11.3.6 (Allmendinger, 2021). Structural data used to create Stereoplots are listed in Table 8, Appendix I.

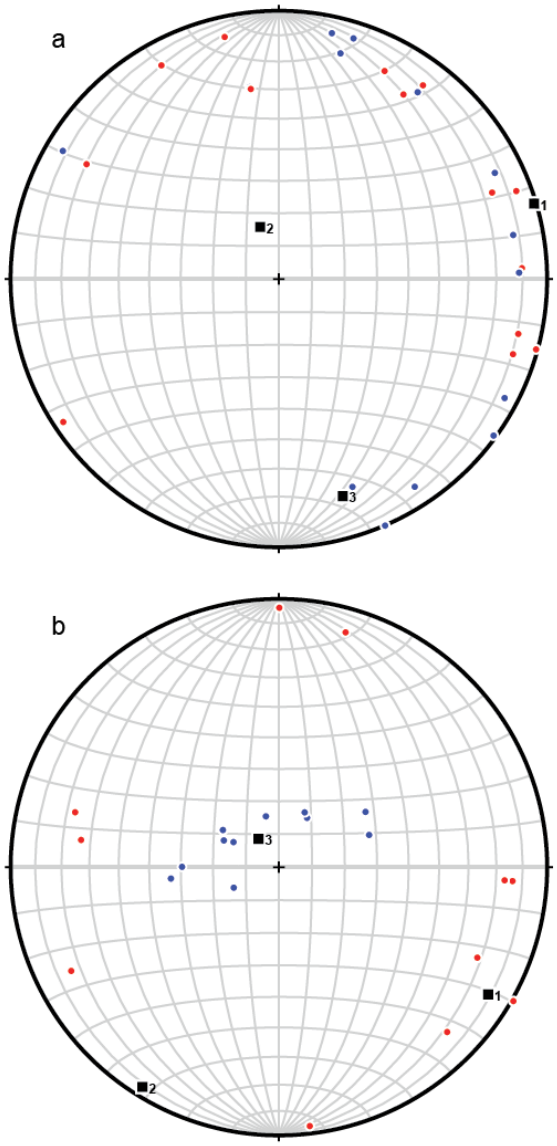

Figure 7. Stereonet scatterplot of P (shortening, blue) and T (extension, red) axes of measured rakes. Principle stress axes indicated by black squares and numbered accordingly. (a) Strike-slip (b) Normal. Stereoplots were made using FaultKin v. 8.1.2 (Allmendinger, 2019). Structural data used to create Stereoplots are listed in Tables 10-11, Appendix I.

CHAPTER 5

Discussion

The San Francisco Mountains have undergone at least two episodes of contraction that have been overprinted by at least four episodes of extension. Shortening structures developed during Mesozoic contraction. Based on cross-cutting relationships with volcanic and sedimentary rocks in the study area, this extension occurred during at least three phases: a Paleocene to Eocene (?) episode that predates volcanic units in the study area and two postvolcanic episodes, one in the Oligocene to Miocene (?) and the other in the Pliocene to Quaternary (?). The general pattern of deformation is consistent with that observed in other nearby ranges that exhibit shortening overprinted by volcanism and extension (Mitra and Sussman, 1997; Friedrich and Bartley, 2003; Yonkee et al., 2019; Pujols et al., 2020). These similarities suggest that the structures in the San Francisco Mountains are the product of regional tectonic events. With the collection of new data and interpretations of the deformational history of the range, along-strike correlations of the Frisco thrust with the Canyon Range thrust and Wah Wah thrust can be better explored. In the following section, spatial and temporal patterns of deformation and regional correlations of structures are discussed in detail.

Mesozoic Contraction

The Frisco Thrust and Related Structures

The Frisco thrust corresponds to the earliest deformation recognized in the San Francisco Mountains. Where the Frisco thrust is exposed, the thrust placed the Precambrian Caddy Canyon Quartzite (Zcc) on top of Paleozoic units. In the northeastern part of the range, the thrust is not exposed and is buried, in places, by the Eocene to Oligocene Horn Silver Andesite (Ths), Paleocene (?) Conglomerate of High Rock Pass (Thr), and Quaternary Alluvium (Qa). The age of the Conglomerate of High Rock Pass (Thr) is debated but nonetheless, thrusting likely occurred before its deposition. The thrust is cut by multiple generations of normal faults and has also experienced shortening in the form of contractional folding, discussed later (Plates 1 and 2).

The Frisco thrust's geometry changes across the range. Moving from west to east, the thrust ramps up across the footwall stratigraphy. Moving from the north to south, the thrust also contains ramps in both the footwall and hanging wall. It is uncertain what unit the thrust lies on outside of the map area, but geometric restorations and area balancing techniques were used to interpret the thrust geometry in the subsurface (Figure 10; Plates 1 and 2).

In the south end of the range, the thrust is well exposed at the surface and makes up the cap of the Frisco Peak. Viewing the thrust in east-west cross-section C-C', the thrust is a flat on the Juab and Wah Wah Limestone (Ojw) and begins to ramp on the stratigraphically higher Kanosh Shale (Ok) and Watson Ranch Quartzite (Owr) (Plates 1 and 2). A balanced restoration of C-C' gives a stratigraphic throw minimum of approximately 5,200 m (Figure 9). The total amount of shortening cannot be determined

because the thrust in the study is a flat and moving to the west, it has been eroded away. It is uncertain where ramps associated with the thrust are located to the west and the east.

In the central part of the range, the thrust crops out on the stratigraphically lower Notch Peak Formation (OCn) in the footwall. The thrust rides the top of the Notch Peak Formation (OCn) as a flat. Cross-section B-B' shows that the thrust is above the Notch Peak Formation (OCn). This ~east-west view of the thrust is slightly oblique in order to highlight extensional structures in the central part of the range. The minimum stratigraphic throw in the center of the range is approximately 4,200 m (Plate 2).

The thrust does not crop out in the northeastern portion of the range. Stratigraphically lower units of the hanging wall of the thrust are exposed in this part of the range that are not observed elsewhere. The Blackrock Canyon Limestone (Zbc) and Pocatello Formation (Zp) hanging wall units are exposed. In cross-section A-A', the thrust can be seen above the Notch Peak Formation (OCn). On the far eastern side of the cross-section, the thrust appears above the Fillmore Formation and House Limestone (Ohf) but has been displaced by extensional structures. The minimum stratigraphic throw is approximately 5,300 m (Plate 2).

Additional thrust structures are observed in the central part of the map area (Plates 1 and 2). Here the Caddy Canyon Quartzite (Zcc) is repeated over the Inkom Formation (Zi), as seen in cross-section B-B' (Plate 2). The repeated section forms a duplex with the Frisco thrust acting as the floor thrust in the duplex. It is unclear if there is only a single horse in the duplex as the top has been eroded away to the east and is likely buried to the west. The duplex is bound by northeast-southwest extensional structures, further distorting its full extent. The stratigraphic throw is at least 600 m, as represented in cross-section B-

B’ (Plate 2), which is small when compared to the throw on the Frisco thrust. The duplex, as well as the Frisco thrust, are folded (Plate 2). Smaller scale folds are recognized in the surface geology on the map (Plate 1). Timing of the duplex is relatively synchronous with that of the Frisco thrust since it cut by the same generations of normal faults and is buried by the Conglomerate of High Rock Pass (Thr). Even with relatively synchronous timing, the duplex thrust must have propagated after the Frisco thrust to have been placed on top of the Frisco thrust.

A network of north-south striking strike-slip faults is observed in the northeastern part of the range, in the hanging wall of the thrust (Plate 1). The strike-slip faults seem to be concentrated in the Blackrock Canyon Limestone (Zbc) and the Caddy Canyon Quartzite (Zcc). Although these faults do crop out occasionally in the stratigraphically higher Mutual Formation (Zm), the Inkom Formation (Zi) does not seem to preserve the faults. This could be due to some lithologic changes between hanging wall units or stress is being concentrated in less competent units like the Blackrock Canyon Limestone (Zbc). This interpretation is supported by small-scale folding observed in the middle and upper member of the Blackrock Canyon Limestone (Zbc) discussed later. The strike-slip faults are not found in any of the footwall units so their timing is likely linked with thrusting. P (shortening) and T (extension) axes were derived from kinematic indicators measured along exposed fault planes. Maximum principle stress ($\sigma_{1)}$ axes yielded a 73° azimuth, thus providing further support to show that the strike-slip faults are kinematically linked with thrusting (Figure 7). Maximum stress orientations were also compared with kinematic indicators measured from normal faults in the area and did not show any relationship with the strike-slip faults. There may have been brief periods where the intermediate principle

stress orientation (σ_2) and minimum principle stress orientation (σ_3) were similar during thrusting allowing the strike-slip faults to form before reverting back to east-west principle stress.

Small-scale folds (one to two m) are found in the hanging wall of the Frisco thrust in the northeastern end of the range. The folds are concentrated in the Blackrock Canyon Limestone (Zbc) members. The Pocatello Formation (Zp) also seems heavily deformed, where exposed, but exposures are limited. Stresses associated with thrusting and exhumation of the Frisco thrust appear to have been concentrated in these less competent limestone and argillite units of the hanging wall. The inferred stress directions are east-west and southeast-northwest. These smaller-scale folds are likely linked with thrusting based on their rock lithologies, strain directions, and closer proximity to the thrust detachment surface.

Late Stage Contraction

There are secondary shortening structures that postdate thrusting recorded in the range. Early interpretations suggested that folding in footwall Paleozoic units occurred prior to thrusting (e.g., East, 1965) but geometric relationships required to restore cross-sections are inconsistent with observations in the hanging wall of the Frisco thrust. Both the footwall and hanging wall of the Frisco thrust are folded by the same structures (Plate 2). These younger folds, which are intermediate to mega-scale structures with wavelengths ranging from 60-1070 m, are more likely related to contraction within the Sevier that post-dates activity along the Frisco thrust.

Geometric relationships link folds in the footwall and hanging wall of the Frisco thrust (Plate 2). A larger synform structure trends northeast through the center of the range.

In cross-section C-C', the Frisco thrust is folded into a synform. The antiform pair to the synform is found to the east and can be restored to the antiform in the footwall via transport along a low-angle normal fault (LANF) discussed in further detail later (Plate 2). The synform continues northeast and appears again in the B-B' cross-section. In B-B', both the Frisco thrust and overriding duplex thrust are folded. Surface dips support this interpretation, and the fold can be traced and matched along the fold hinge moving northeast from C-C' to B-B' (Plate 2). The dip panel in cross-section view dips to the east in C-C'. Moving to the northeast in B-B', the dip panel also dips to the east but the surface units on the southeastern portion of the cross-section dip west. This could be due to the matching antiform structure being located out of the map area to the east, an area that is presently covered by the Eocene to Oligocene Horn Silver Andesite (Ths). Displacement along a LANF can account for the movement. Similarly, the synform structure in the northwestern portion of B-B' would be traced to out of the mapping area and buried in the Wah Wah Valley, directly west of the San Francisco Mountains. The minimum amount of shortening associated with this structure is 70 m. This measurement is taken from the change in length of the deformed and retrodeformed cross-section C-C' (Figure 9). Total amount of shortening from these structures is unknown because of the incomplete exposure or erosion.

Cenozoic Extension

Low-Angle Normal Faults (LANF)

The oldest extensional structure documented in the study area is a low-angle normal fault (LANF) in the northeastern part of the range (Plate 1). The fault is positioned at the

upper contact of the middle member of the Blackrock Canyon Limestone (Zbcd). The fault excises the upper member of the Blackrock Canyon Limestone (Zbcu) and placed the Blackrock Canyon Limestone middle member (Zbcd) in direct fault contact with the stratigraphically higher Caddy Canyon Quartzite (Zcc). Lemmon and Morris (1984) mapped the fault as a stratigraphic contact; however, their interpretation does not account for the 50 m of the Blackrock Canyon Limestone upper member (Zbcl) that is missing and can be found in outcrop farther north in the map area (Plate 1). Cross-section restorations indicate that the faults originally dipped to the west but have since been rotated to its current orientation by younger normal faults giving the fault an apparent eastward dip. Extension associated with this LANF likely closely followed thrusting and contraction since the thrust and the LANF both have apparent dips to the east. The fault is also cut by younger normal faults and thus, predates much of the Miocene to Quaternary extension in region.

A balanced restoration of cross-section A-A' results in a minimum heave of 1,000 m along the LANF (Figure 8). To the west, the fault displaces the strike-slip faults and eventually reaches and most likely merges with, but does not cut, the Frisco thrust, as shown in the northeastern end of cross-section D''-D''' (Plate 2). To the east, the fault continues out of the map area. Total displacement is unknown since the fault feeds into the Frisco thrust and reactivated it. The LANF cuts down in stratigraphic section and appears again on the map to the west of its original contact (Plate 1). Where the fault outcrops again, it is in the Blackrock Canyon Limestone lower member (Zbcl). This is both consistent with map pattern and cross-section A-A' where the LANF is in the subsurface on the same corresponding stratigraphic unit.

There is another set of LANF's in the southwest of the range (Plate 1). The lower of two LANF's in this area placed the Notch Peak Formation (OCn) in contact with the Big Horse Limestone (Cob) and effectively removes the full thickness of the Steamboat Pass Shale (Cosp). A thick (five to ten m) gouge zone can be observed at this contact. A higher LANF placed a thin sliver of Fillmore Formation and House Limestone (Ohf) above the Notch Peak Formation (OCn). This fault cuts out part of the Fillmore and House Limestone (Ohf). These LANF's were originally mapped as thrust faults by Hintze et al. (1984), likely based on their low-angle geometry and missing strata at these locales. However, the clear younger over older relationships suggest otherwise. Alternatively, the low-angle feature could be stratigraphic contacts; however, such an interpretation does not account for the 60 m of Steamboat Pass Shale (Cosp) and over 400 m of the Fillmore and House Limestone (Ohf) that are missing. Both of these faults dip to the east and have been steepened due to the recent tilting of the range. These faults appear to have initiated after the LANF documented at the northern end of the range as the faults dip to the east and tie into the cross-sections in the north with the area balance D-D' and D''-D''' (Figure 10; Plate 2). The LANF's do not cut any of the high-angle normal faults.

Retrodeformable cross-section C-C' accounts for movement along the faults (Figure 9). Minimum displacements were used to balance the cross-section. For the lower fault (OCn on Cob), there is a minimum heave of 420 m. The upper LANF has a greater heave of 3,650 m. The faults move out of the map area to the east. Viewing the fault moving to the northeast in cross-section D-D' and D''-D''', the lower fault meets with the less competent Steamboat Pass Shale (Cosp) and merges into the larger LANF above. Geometric relationships and the small amount of displacement in this view were the cause

for this interpretation. The higher LANF cuts down stratigraphic section to the north. Displacement increases along the fault to the northeast until it eventually merges with the Frisco thrust (Plate 2). The fault can be traced into cross-section A-A' where the retrodeformed section was used to estimate heave (Figure 8). Heave in the northeast is up to 8,100 m. Total displacement is unknown if the LANF feeds into the Frisco thrust and causes thrust reactivation. Total displacement on the LANF's is consistent with fault length-displacement ratios discussed in Gudmundsson (2013).

High-Angle Normal Faults

Prevolcanic Paleocene to Eocene (?) high-angle faults are the most abundant faults in the range. Based on fault strikes and cross-cutting relationships among the faults, several prevolcanic fault sets are recognized. The first is a set of north-south-striking normal faults, found in the southern and northern parts of the range (Plate 1). The faults cut the Frisco thrust and related strike-slip faults, and the LANF's. However, these faults do not cut any Cenozoic units and are not cut by any other normal fault sets. Their relative timing could be linked with that of the larger northeast-southwest faults but it is unclear where the faults abut due to burial in Quaternary Alluvium (Qa). It is also possible that these faults are linked to the much younger north-south faults that do cut Cenozoic units, discussed later, but it is unlikely because that would have required all of the Cenozoic volcanic units to be eroded away where these faults are exposed. These faults cut both the hanging wall and footwall units of the Frisco thrust. Stratigraphic separations range from 100 to 900 m in the north, and a minimum of 60 m in the south.

The next set of prevolcanic Paleocene to Eocene (?) faults are relatively large northeast-southwest striking faults. These faults are exposed throughout the range but are

most prevalent in the center of the range (Plate 1). The faults cut the Frisco thrust, the duplex thrust, the LANF's, and the other high-angle normal fault sets or rather the other high-angle normal fault sets abut into these larger faults. Confined between these faults are sets of northwest-southeast striking faults and a set of north-south striking faults. The timing of the confined faults is likely synchronous with the northeast-southwest faults because they cannot be traced on the other sides of the northeast-southwest faults. None of these faults cut Cenozoic units but they are buried by them. The faults mainly occurred in the hanging wall of the Frisco thrust and have minimum stratigraphic separations of 40 m. The larger northeast-southwest faults have stratigraphic separations ranging from 300 to 800 m.

Cross-section B-B' highlights the northeast-southwest extensional structures as the section line is roughly perpendicular to their strike (Plate 2). Looking at the faults in cross-section view B-B', the faults confine the duplex thrust between them. Stratigraphic section is repeatedly dropped to the west as smaller high-angle normal faults feed slip into the larger northeast-southwest strands. To the west, the duplex is also displaced and the repeating section is buried with Mutual Formation (Zm) exposed at the surface. To the east the duplex structure was exhumed and eroded as the contact with the Frisco thrust is exposed on the southeast end of the cross-section with Caddy Canyon Quartzite (Zcc) thrust on the Notch Peak Formation (OCn).

There is at least one set of postvolcanic Oligocene to Miocene (?) high-angle normal faults. The faults strike north-south and are found in the southern end of the range (Plate 1). The faults cut the Horn Silver Andesite (Ths) and juxtapose the volcanic units against footwall and hanging wall rocks of the Frisco thrust. The faults are not well exposed

and may be more abundant to the east of the range where volcanic units are more prevalent. Poor exposure could also be due to the weathering pattern of the Horn Silver Andesite (Ths), which has multiple lithologies including ash-flow tuffs that may not record deformation as well as more lithified rocks. It is possible that the previously mentioned larger strands of north-south faults belong to this fault set, but it is unlikely that erosion would have exposed these faults in the southwest end of the range and not the southeast end of the range. Stratigraphic separation for these faults is unknown since both the Conglomerate of High Rock Pass (Thr) and the Horn Silver Andesite (Ths) have widely varying and uncertain thicknesses.

The Pliocene to Quaternary (?) high-angle normal faults are mainly range-bounding faults buried in Quaternary alluvium (Qa). The faults strike northeast-southwest and only appear on the edges of the map area (Plate 1). These faults are not well exposed but scarps are present in aerial imagery in alluvium. Also, juxtaposition of klippen surrounded by alluvium suggest that there must be faults in the area to stratigraphically drop down higher rock units. These faults are contributing to Basin-and-Range east-west extension. These faults also likely contributed, or are still contributing, to the up to 15° tilting of the range. Tilting of the range has made the normal faults sets appear to have steeper dip than their initiation dips. The Conglomerate of High Rock Pass (Thr) has a couple of recorded dips, from 12° to 16° to the west. The age of this conglomerate is debated and may be synorogenic, but assuming the conglomerate was deposited after thrusting, these dips can be used to estimate the amount of tilting in the range. The stratigraphic throw of these faults is unknown.

Along-Strike Thrust Correlations

The San Francisco Mountains and the Frisco thrust are part of the larger regional contraction of the Sevier fold-thrust belt (DeCelles, 2004; DeCelles and Coogan, 2006). The Sevier fold-thrust belt is characterized by multiple thrust sheets with different magnitudes of shortening, structural styles, and timing (Mitra and Sussman, 1997; Friedrich and Bartley, 2003; Yonkee et al., 2019; Pujols et al., 2020). The Frisco thrust lies between the better studied Canyon Range-Willard thrust sheet to the north and the Wah Wah thrust sheet to the south although along-strike correlations and evolution of the Frisco thrust are not well established (Anders et al., 2012). New data reveals some constraints on the structural style of the Frisco thrust sheet discussed previously. These new geometric data can be used to compare the Frisco thrust with the Canyon Range-Willard sheet to the north and the Wah Wah thrust sheet to the south. Inferences can be made about along-strike correlations and implications of the different thrust sheets.

Willard Thrust

The Canyon Range-Willard thrust sheet to the north of the Frisco thrust is broken up into two correlative segments. The Willard thrust, in the Monte Cristo Range, placed Precambrian Browns Hole Formation and the lower Cambrian Geertsen Quartzite on top of Triassic to Jurassic sedimentary rocks (Dover, 2007; Yonkee et al., 2019). The Precambrian Browns Hole Formation is a thin siltstone that sits stratigraphically on top of the Mutual Formation (Zm) and is not present or differentiated south of the Willard thrust in Utah. The lower Cambrian Geertsen Quartzite is believed to be equivalent to the Cambrian Prospect Mountain Quartzite (Cpm) found in the San Francisco Mountains. The

Geertsen Quartzite sits stratigraphically above of the Mutual Formation (Zm) and will be referred to as the Prospect Mountain Quartzite (Cpm) from herein after when referencing the Willard thrust. The Willard thrust footwall ramps up section, from Paleozoic in the west to Mesozoic rocks to the east. It also contains a ramp in its hanging wall, from the Paleozoic down to the Mutual Formation (Zm). There appear to be flats in the hanging wall beneath the Mutual Formation (Zm) but the geology is uncertain. The Willard thrust accommodates 60 km of shortening (Yonkee et al., 2019). Duplex structures seem to absent or are not recognized in the thrust geometry. The footwall is folded by blind thrusts to the east of the Willard thrust. The hanging wall and thrust are folded but folds in the hanging wall do not seem to be linked with footwall folds.

Canyon Range Thrust

The second segment of this thrust pair, the Canyon Range thrust, is folded into a tightly hinged synform where exposed. The synform is a result of the successive growth of an antiformal stack that developed to the west of the synform exposure of the Canyon Range thrust (Sussman, 1995; Sussman and Mitra, 1995). Reconstructions of the Canyon Range thrust have been interpreted as having a forward-breaking thrust sequence in its footwall (Mitra and Sussman, 1997). The thrust placed Pocatello Formation (Zp) and Blackrock Canyon Limestone (Zbc) over the undifferentiated Ordovician Pogonip Group (Kanosh Shale (Ok), Juab and Wah Wah Limestones (Ojw)), and the Fillmore and House Limestones (Ohf) in the west. In the east, the Canyon Range thrust placed Pocatello Formation (Zp), Blackrock Canyon Limestone (Zbc), and Caddy Canyon Quartzite (Zcc) over Devonian to Cretaceous sediments (Mitra and Sussman, 1997; Stockli et al., 2001; Hintze and Davis, 2002; DeCelles and Coogan, 2006; Pujols et al., 2020). The Canyon

Range thrust ramps up section, from Devonian rocks in the east to Cambrian rocks in the west. The hanging wall also ramps from Caddy Canyon Quartzite (Zcc) in the east down to Pocatello Formation (Zp) in the west. It is not quite clear where the hanging wall flats occur within the section. The Canyon Range thrust accommodates 100 km of shortening. Folding of the Canyon Range thrust and its footwall was caused by the lower Pavant thrust sheet (Mitra and Sussman, 1997; DeCelles and Coogan, 2006).

Wah Wah Thrust

To the south of the Frisco thrust lies the Wah Wah thrust. The Wah Wah thrust is folded into a more broadly hinged synform structure. Reconstructions of the Wah Wah thrust have been interpreted as having a backward-breaking sequence in its footwall. The sequence is derived from balanced cross-sections of the Wah Wah thrust and the six imbricate thrusts that make up the Wah Wah Mountains. (Friedrich and Bartley, 2003). The thrust placed Pocatello Formation (Zp) over undifferentiated Paleozoic strata in the west and Caddy Canyon Formation (Zcc) over Mississippian and Pennsylvanian sediments to the east (Miller, 1966; Abbott et al., 1983; Friedrich and Bartley, 2003). The footwall of Wah Wah thrust ramps up section, from Mississippian rocks in the west to Pennsylvanian rocks to the east. There is a hanging wall ramp from the Caddy Canyon Quartzite (Zcc) in the east down to Pocatello Formation (Zp) in the west. A hanging wall flat appears to occur in the Pocatello Formation (Zp) in the west but the stratigraphy is buried to the west so relationships become uncertain. A hanging wall flat was chosen at a point to minimize thrust displacement. The Wah Wah thrust accommodates 38 km of shortening (Friedrich and Bartley, 2003). There is folding in the hanging wall of the Wah Wah thrust that was caused by underlying imbricate thrusts in the range. The absence of lateral variations of

deformation in the Wah Wah syncline provides more support that the Wah Wah thrust was emplaced by a backward-breaking thrust sequence (Friedrich and Bartley, 2003).

Frisco Thrust

Where exposed, the Frisco thrust placed Caddy Canyon Quartzite (Zcc) on Paleozoic sedimentary rocks (Plate 1). There is a hanging wall ramp cutting up in section from the Pocatello Formation (Zp) in the north to the Caddy Canyon Quartzite (Zcc) in the south (Plate 2). The thrust is ramping up in footwall section to the east. Total amount of shortening cannot be determined because of the absence of a hanging wall ramp to the west. There is a duplex structure in the center of the range. The duplex is structurally higher than the older Frisco thrust below in cross-section B-B' (Plate 2). This suggests a backward-breaking sequence of thrusting in the range since the duplex thrust is structurally higher and must have propagated after the Frisco thrust. The thrust is folded into a gentle synform structure in the southern part of the range. Folding of the thrust is linked to post-thrusting contractional events.

Although the thrust correlations are not clear due to limited exposures, inferences can be made about along-strike thrust correlations of the Frisco thrust. The sequence of thrusting is consistent with the backward-breaking sequence of the Wah Wah thrust and not the forward-breaking sequence of the Canyon Range thrust. The Frisco thrust has a stratigraphic throw of approximately 4,200 m to 5,300 m. The total amount of throw for the Frisco thrust is close with that of the Wah Wah thrust, approximately 5,200 m to 5,800 m (Abbott et al., 1983). By comparison, the Canyon Range has a stratigraphic throw of greater than 7,500 m but the subsurface rocks are lumped together with unknown thicknesses in some parts of the stratigraphy (Hintze and Davis, 2002). Given the amount

of stratigraphic throw, it is more likely that the total amount of shortening for the Frisco thrust is closer to the 38 km of shortening on the Wah Wah thrust (Friedrich and Bartley, 2003) compared to the much larger 100 km of shortening on the Canyon Range thrust (Mitra and Sussman, 1997; DeCelles and Coogan, 2006) even though total shortening for the Frisco thrust could not be determined. On the other hand, the Frisco thrust displays a footwall ramp through Ordovician units which is displayed in the Canyon Range thrust. The Wah Wah thrust has a footwall ramp through Mississippian and Pennsylvanian units.

There are problems with directly correlating the Frisco thrust with both the Wah Wah thrust and the Canyon Range thrust. The Wah Wah thrust and accompanying imbricate thrusts are all placed over Mississippian and Pennsylvanian rocks whereas the Frisco thrust is placed over Cambrian and Ordovician rocks. Corrugations or a ramp in the thrust geometry between the Wah Wah Mountains and the San Francisco Mountains could serve as an explanation for the difference in stratigraphic throw, but it is unknown what structures lie in the Wah Wah Valley that separates the ranges. Folding in both the Wah Wah thrust and Canyon Range thrust has been interpreted as synchronous with thrusting (Mitra and Sussman, 1997; Friedrich and Bartley, 2003; DeCelles and Coogan, 2006) while folding of the Frisco thrust is likely more related to post-thrusting contraction. The Frisco thrust shows geometry in the thrust from the north end of the range to the south end in the form of a hanging wall ramp cutting up section to the south. Both the Wah Wah thrust and the Canyon Range thrust do not seem to share this geometry.

Synthesis

The San Francisco Mountains are host to a number of structures that formed during multiple stages of deformation. Mesozoic contraction has been later overprinted by at least

four episodes of extension that can be separated into three different time intervals: prevolcanic Paleocene to Eocene (?), postvolcanic Oligocene to Miocene (?), and Pliocene to Quaternary (?) episodes (Plate 1). Contraction is represented by the east vergent Frisco thrust that placed Precambrian rocks on top of Paleozoic rocks. The thrust ramps laterally from north to south. Hanging wall ramps are exposed to the east but not in the west. A backward-breaking duplex exposed in the center of the range reveals repeating Precambrian section. After some period of quiescence, extensional faults began to disrupt the thrust within the range. Prevolcanic Paleocene to Eocene (?) extension is represented by several sets of normal faults with different relative timing. Two separate sets of low-angle normal faults, previously mapped as thrust faults (Hintze et al., 1984), are recorded cutting out thickness in footwall units. The range was then further extended by sets of high-angle normal faults that do not cut Cenozoic units. Postvolcanic Oligocene to Miocene (?) high-angle normal faults cut through the Eocene to Oligocene Horn Silver Andesite (Ths). A final set of range-bounding faults from Pliocene to Quaternary (?) have tilted the range to its current orientation.

Extensional fault sets have different relative timing due to changes in stress regimes over time. It has been shown on a larger scale how the changing plate margin on the west coast has changed stress regimes of the Western United States Cordillera (McQuarrie and Wernicke, 2005). This model can be directly applied and observed in the San Francisco Mountains where different striking normal faults contribute to several episodes of Basin-and-Range extension. Given the different orientation of faults in the range, the stress field on the San Francisco Mountains reoriented at least five times throughout its history of contraction and extension.

It is unclear as to which thrust sheet the Frisco thrust belongs to. New data suggest that the Frisco thrust is more closely related with the Wah Wah thrust than the Canyon Range-Willard thrust due to their similar structural style, but other problems prevent a direct correlation. Incomplete exposures of buried and eroded hanging wall section also do not assist in correlation. Differences in interpretation of deformation, namely timing of folding, do not precisely align the Frisco thrust with the correlative options.

Improvements to the Map

Several improvements to the existing published maps have been made by the newly collected map data. The original mapping was completed at 1:48,000 scale, the new map is completed at 1:24,000 scale. The finer scale allows for more geometric and kinematic data to be represented within the map area. Additionally, faults and fault sets have been distinguished at the finer scale. Fault relationships that were originally interpreted as multiple thrust faults but have clear younger over older relationships have been assessed and reinterpreted as low-angle normal faults. Not only does this reconcile stratigraphic relationships across the faults, but this also reconciles unit thickness discrepancies between published maps. Cross-cutting relationships between separate generations of fault sets have been re-evaluated and clarified. Multiple generations of extensional structures have been identified with the assistance of structural analysis. The recognition of a duplex structure has been identified in the center of the range. This suggests a more complicated contractional history and may help with along-strike correlations. Geologic contacts have been refined and more precisely determined using GPS enabled tablets. Quaternary units have been differentiated using National Agriculture Imaging Program (NAIP) imagery.

Improvements result in a higher resolution geologic map with more clear structural relationships.

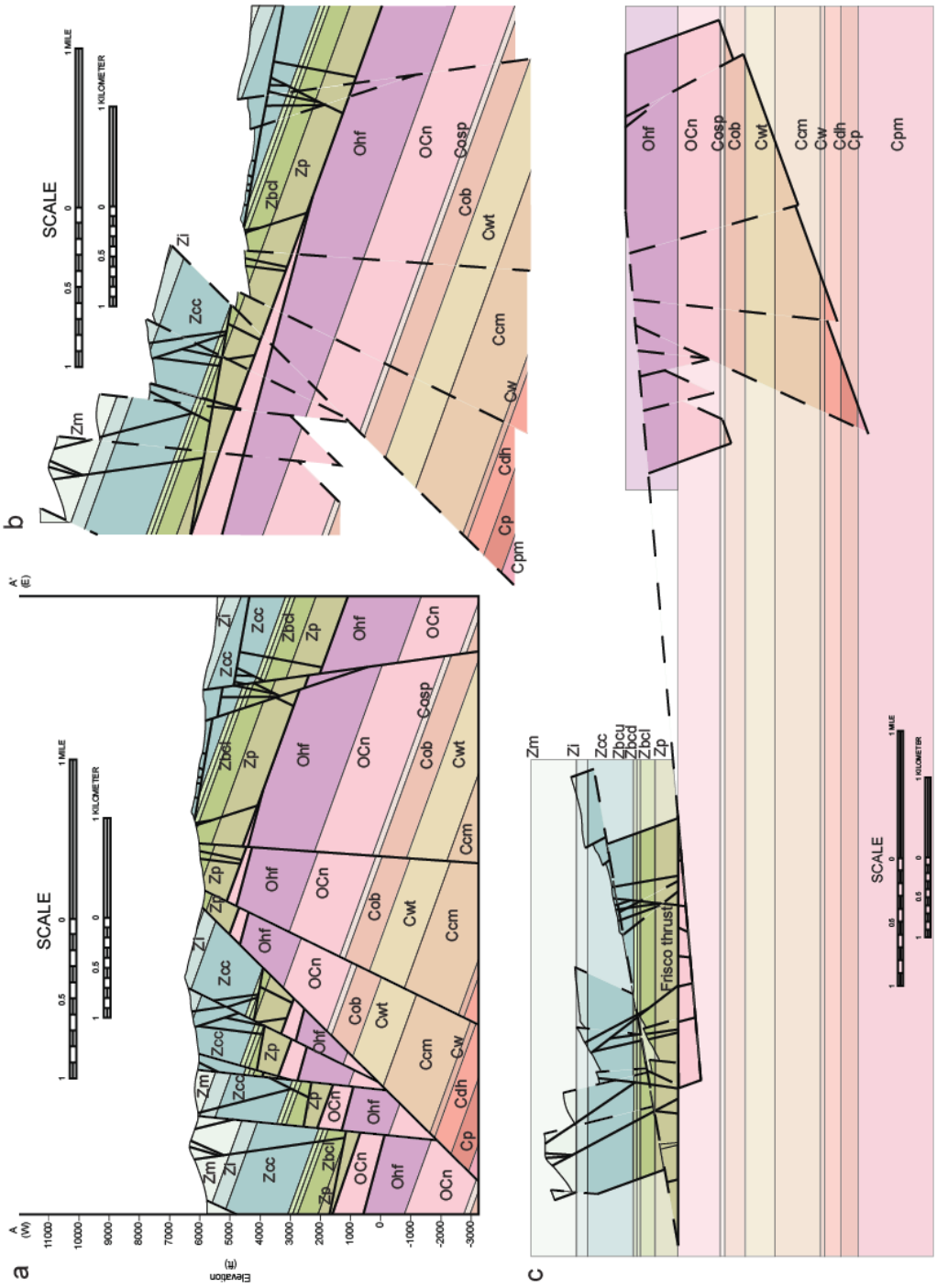

Figure 8. Restored and balanced cross-section A-A'. (a) Deformed state, (b) high-angle faults restored, (c) low-angle faults restored.

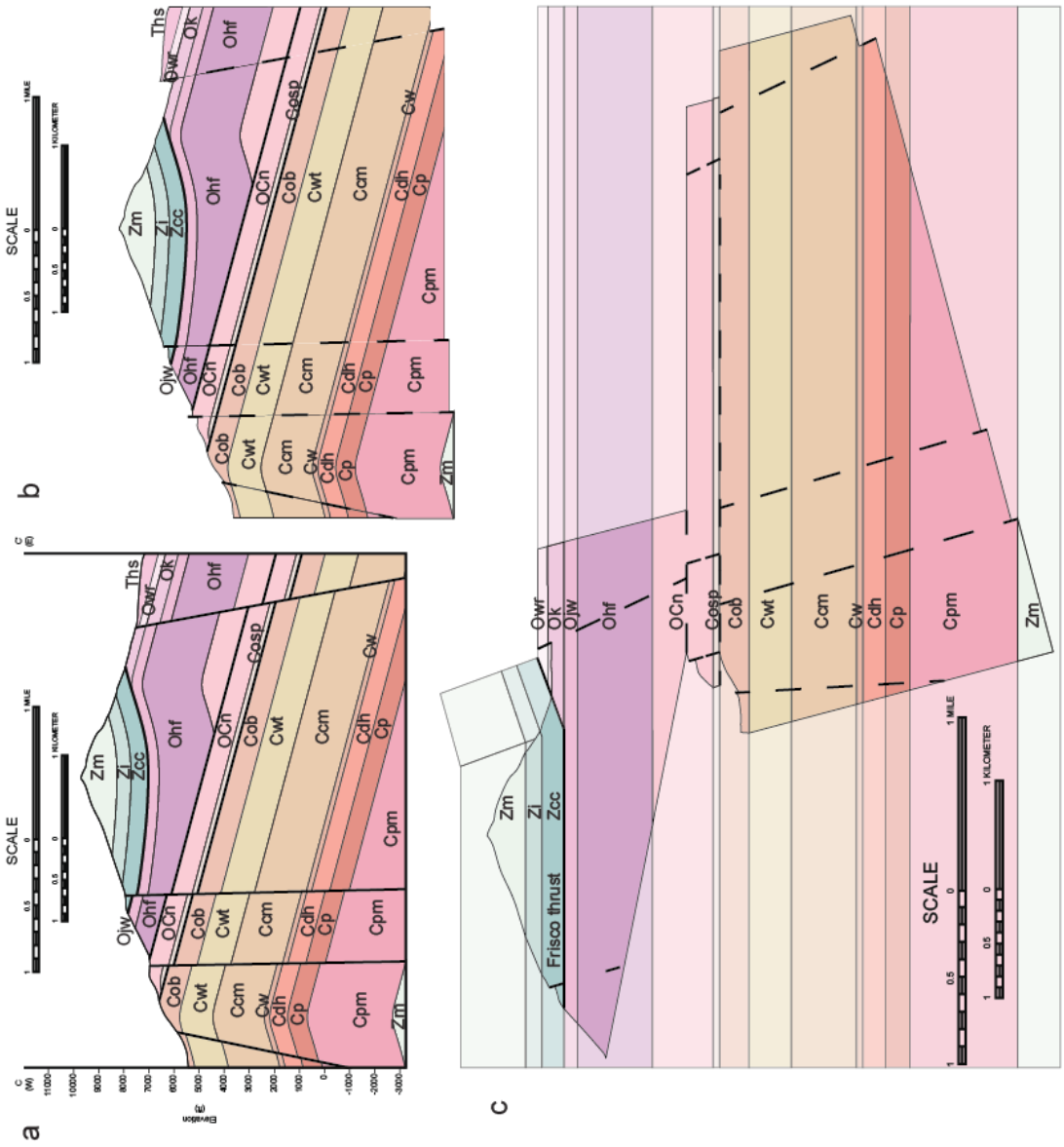

Figure 9. Restored and balanced cross-section C-C'(a) Deformed state, (b) high-angle faults restored, and (c) low-angle faults restored.

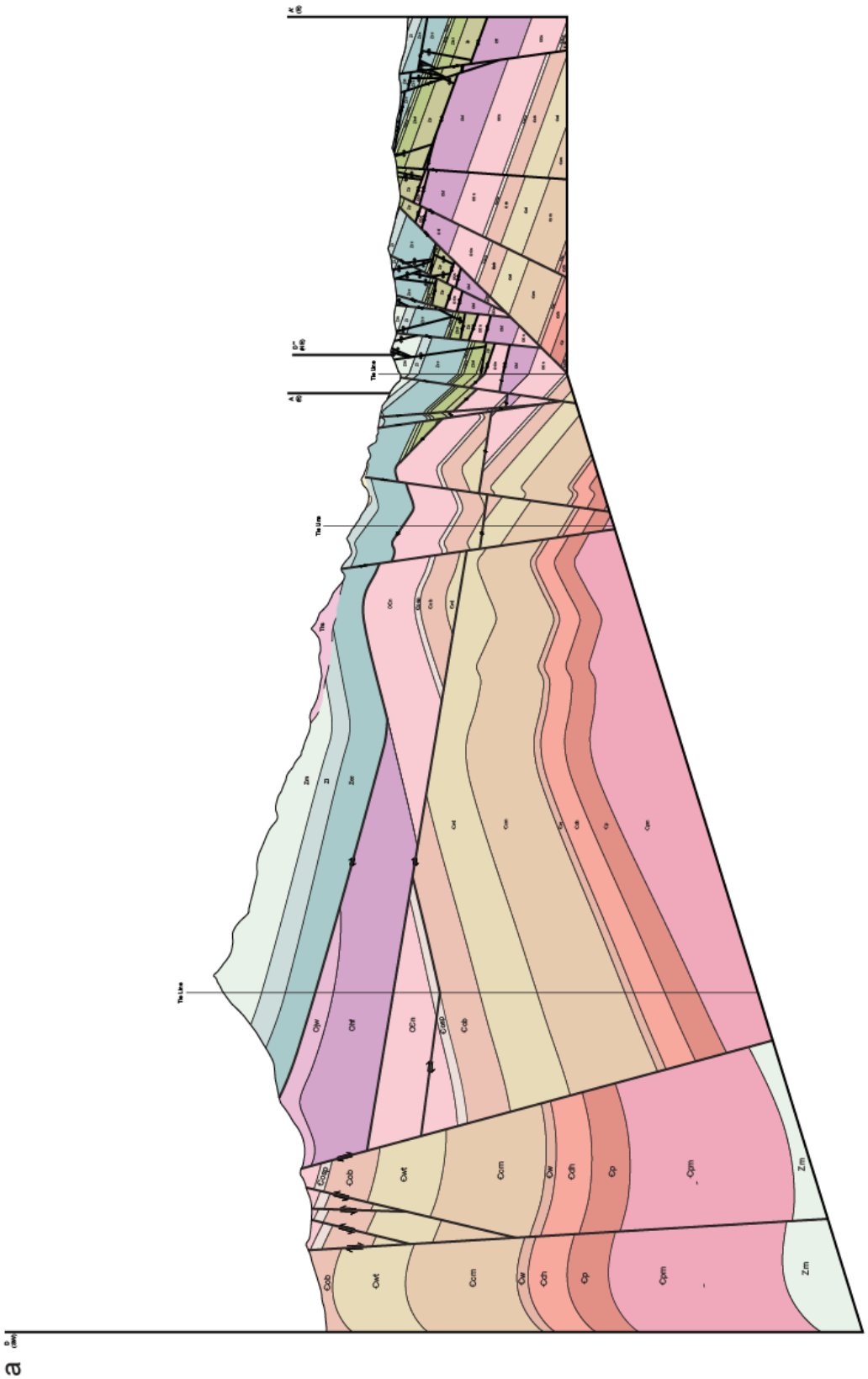
a

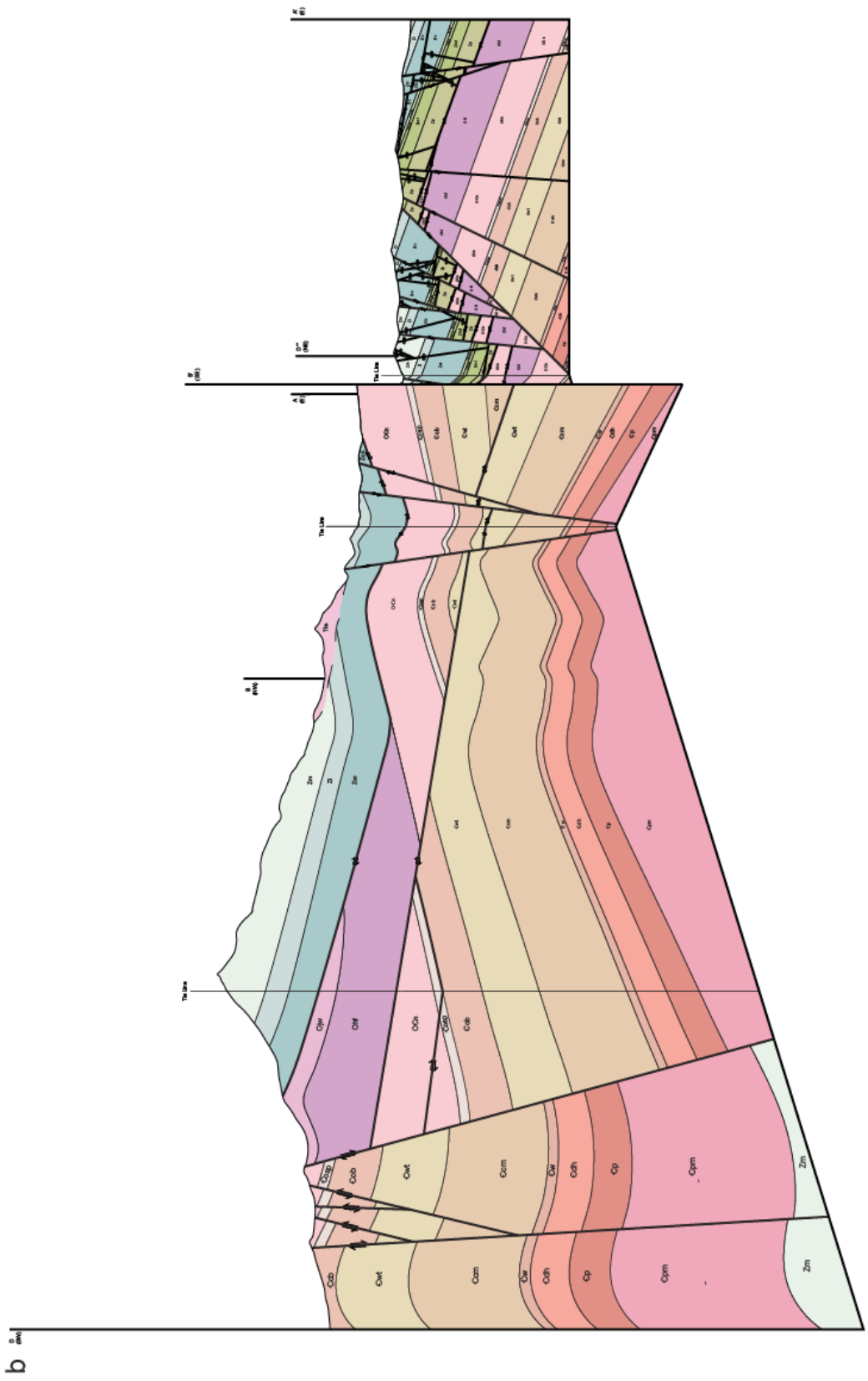
b

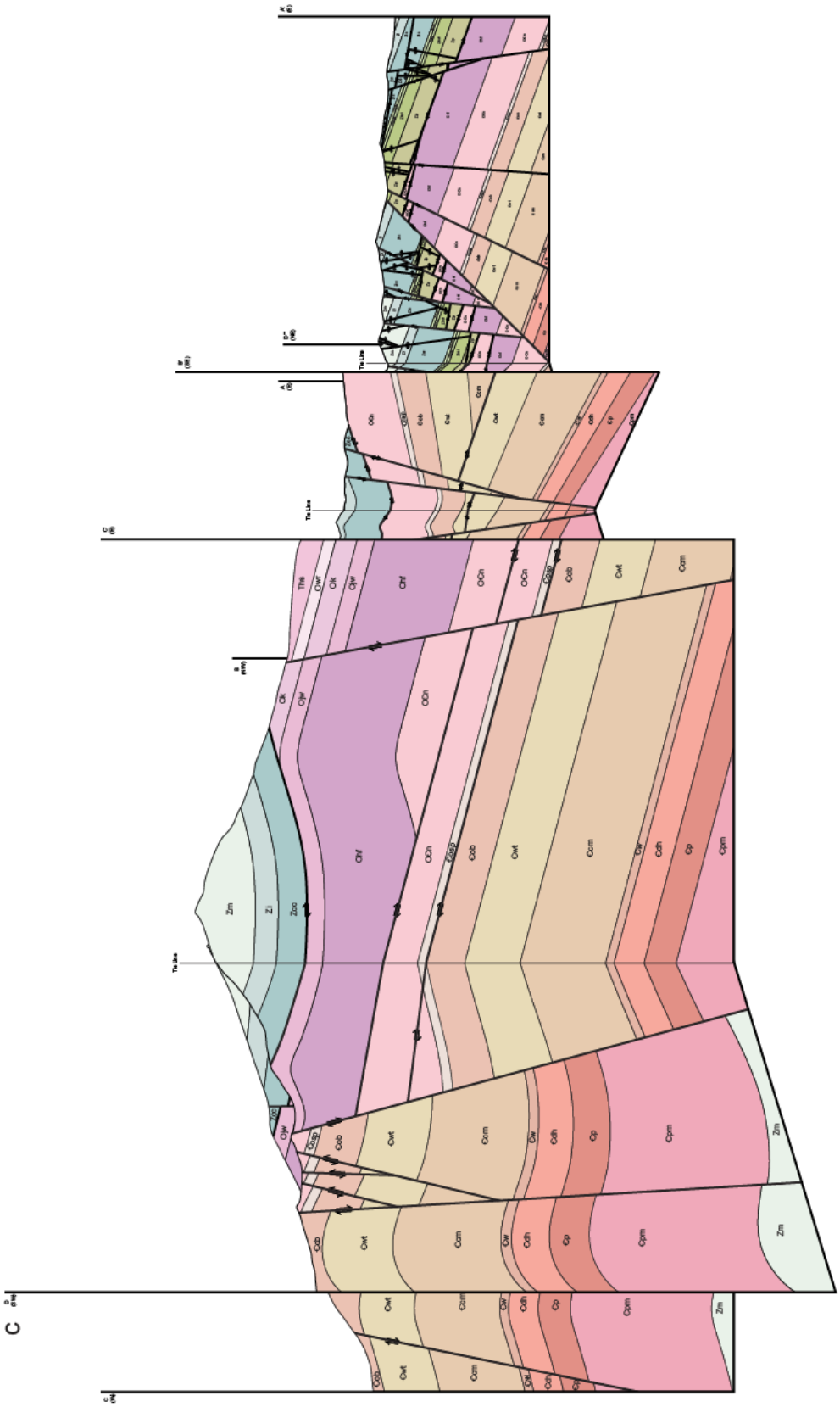
C

Figure 10. Fence diagram of cross-sections showing three-dimensional interpretation of subsurface geology (view to the northeast from the southern end of the range). Separated into three sections (a) without B-B' and C-C', (b) without C-C', (c) with all cross-sections.

CHAPTER 6

Conclusion

The Sevier fold-thrust belt presents challenges of interpreting and correlating along-strike shortening structures that have been overprinted by extension. This study collected new detailed (1:24,000 scale) geologic map data in the San Francisco Mountains where the new map data was used to construct balanced cross-sections and an area balance of the range. The cross-sections were used to constrain the geometry, structural style, and relative timing of deformation of the range in three dimensions.

New map data reveal structures of the deformational history although field relationships of faults are not always apparent. The deformation can be separated into five events beginning with Mesozoic contraction. (1) The Frisco thrust sheet shows changing geometry along-strike. The thrust ramps up in hanging wall and footwall sections to the south along-strike. Across-strike, an eastern ramp up the footwall section is observed but where the ramp is located to the west in uncertain. A structurally higher duplex thrust is preserved in the center of the range suggesting a backward-breaking style of thrusting. (2) Two separate sets of low-angle normal faults. The first in the north end of the range cutting out the Blackrock Canyon Limestone upper member (Zbcu). The second set in the south end of the range cutting out thickness of the Fillmore Formation and House Limestone (Ohf) and completely cutting out the Steamboat Pass Shale (Cosp). (3) Prevolcanic high-angle normal faults cut the earlier fault sets but not Cenozoic units found in the range. (4) High-angle faults cut the approximately 30 Ma Horn Silver Andesite (Ths). (5) The

youngest range-bounding faults cut all earlier fault sets and contribute to tilting of the range to its current orientation.

Extensional overprint also makes along-strike correlations unclear. Evidence suggests that the Frisco thrust is correlated with the Wah Wah thrust due to its backward-breaking structural style. However, the Frisco thrust relationship with the Canyon Range-Willard thrust is uncertain and cannot be dismissed. The relationship between thrusts is not definitive as interpretations of timing of deformation and juxtaposition of hanging wall and footwall rocks between the ranges does not coincide. The thrust and underlying units contain corresponding folds that occurred as a result of post-thrusting contraction in the San Francisco Mountains while folded is interpreted as synchronous with thrusting in the Wah Wah Mountains and Canyon Range. The Frisco thrust placed Precambrian over Cambrian and Ordovician which is seen in the Canyon Range thrust. In contrast, the Wah Wah thrust placed Precambrian over Mississippian and Pennsylvanian. These contradictions make definitive thrust correlations uncertain.

Future Work

A thermochronology transect was collected in the San Francisco Mountains (Appendix III, Figure 11). Samples have been processed down to mineral separates and are awaiting analysis. These thermochronology data will allow for quantitative constraints on the exhumation of the hanging wall of the Frisco thrust. While there is no published timing data for the Wah Wah thrust, there is published timing data from the Canyon Range-Willard thrust. For complete thrust correlations, timing data along with the structural data from all three thrust sheets would be needed to define thrust relationships.

APPENDICES

Appendix I

Analytical Data

TABLE 1. PLANES TO POLES
THRUST FAULTS

Fault	Strike	Dip (RHR)
1	126	17
2	171	19
3	229	10
4	150	11
5	236	4
6	203	35
7	195	7
8	193	12
9	190	11
10	192	7
11	228	16
12	99	26
13	99	7

Note: RHR= right hand rule.
Used for Figure 5.

TABLE 2. POLES TO PLANES
STRIKE-SLIP FAULTS

Fault	Strike	Dip (RHR)
1	36	80
2	230	77
3	43	54
4	221	88
5	189	74
6	205	78
7	202	69
8	235	75
9	18	68
10	318	84
11	242	84
12	138	86
13	188	70
14	236	86
15	64	65
16	173	89
17	168	80
18	164	76
19	171	60
20	162	80
21	11	88
22	242	86
23	149	79
24	178	71
25	90	76
26	182	89
27	170	60
28	243	83
29	185	78
30	178	82
31	192	85
32	179	66
33	179	79
34	239	81
35	171	83
36	198	90

Note: RHR= right hand rule.
Used for Figure 5.

TABLE 3. POLES TO PLANES
LOW-ANGLE NORMAL FAULTS

Fault	Strike	Dip (RHR)
1	38	9
2	296	6
3	26	9
4	10	12
5	63	27
6	13	15
7	313	22
8	41	23
9	358	12
10	109	4
11	132	22
12	72	17
13	91	6
14	131	18

Note: RHR= right hand rule.
Used for Figure 5.

TABLE 4. POLES TO PLANES
NW-SE FAULTS

Fault	Strike	Dip (RHR)	Fault	Strike	Dip (RHR)
1	340	87	22	151	89
2	253	62	23	143	67
3	246	70	24	148	51
4	246	50	25	110	58
5	340	83	26	116	86
6	262	77	27	143	52
7	318	87	28	117	50
8	300	62	29	74	78
9	265	76	30	157	88
10	277	82	31	128	87
11	286	54	32	153	87
12	279	78	33	120	62
13	320	51	34	142	48
14	334	89	35	105	42
15	271	67	36	111	56
16	328	65	37	336	54
17	293	48	38	326	41
18	302	41	39	258	79
19	305	67	40	120	46
20	270	61	41	131	84
21	267	42	42	254	86

Note: RHR= right hand rule.
Used for Figure 5.

TABLE 5. POLES TO PLANES
NE-SW FAULTS

Fault	Strike	Dip (RHR)
1	51	62
2	49	82
3	25	83
4	45	88
5	212	58
6	24	47
7	211	79
8	44	85
9	36	74
10	225	53
11	246	70
12	246	50
13	224	63
14	235	65
15	43	88
16	51	61
17	50	60
18	51	61
19	206	85
20	221	87
21	228	81
22	212	71
23	230	74
24	65	31
25	210	55
26	214	47
27	33	83
28	209	50
29	233	40
30	211	31
31	13	56
32	18	79

Note: RHR= right hand rule.
Used for Figure 5.

TABLE 6. POLES TO PLANES
N-S FAULTS 1

Fault	Strike	Dip (RHR)
1	340	87
2	345	79
3	178	74
4	190	71
5	162	82
6	355	77
7	340	83
8	354	71
9	351	88
10	200	77
11	355	88
12	16	54
13	343	57
14	183	82
15	197	85
16	5	69
17	360	78
18	191	61
19	193	84

Note: RHR= right hand rule.
Used for Figure 5.
Blue poles in southern part of range.

TABLE 7. POLES TO PLANES N-S FAULTS 2

Fault	Strike	Dip (RHR)
1	186	85
2	14	88
3	191	73
4	175	31
5	196	73
6	357	49
7	347	75
8	193	58
9	171	39
10	18	79
11	193	56
12	342	58
13	7	84
14	183	77
15	357	80
16	18	65
17	348	86
18	8	88
19	354	42

Note: RHR= right hand rule.
Used for Figure 5.
Red poles in central part of range.

TABLE 8. PLANES TO PI-AXES

Fold	Strike	Dip (RHR)
1	280.7	88.2
2	34.7	86.8
3	175.6	88.3
4	121.1	86.7
5	341.3	89.6
6	250.4	87.2
7	96.5	84.4
8	153.6	89.6
9	162.7	85.6
10	346.2	88.3
11	93.4	86.8
12	137.4	52
13	333.6	77.5
14	128.5	84.2
15	95.2	86.6

Note: RHR = right hand rule.
Used for Figure 6.

TABLE 9. MEASURED FAULTS

Fault	Strike	Dip (RHR)	Rake	Fault	Strike	Dip (RHR)	Rake
1	340	87		44	221	88	15S
2	345	79		45	51	61	81N
3	151	89		46	50	60	37N
4	178	74		47	51	61	
5	190	71		48	228	81	
6	162	82		49	205	78	14N
7	355	77		50	212	71	
8	340	83	78N	51	165	64	
9	262	77		52	13	75	
10	318	87	83E	53	230	74	
11	200	77		54	202	69	33S
12	355	88		55	235	75	64S
13	213	54		56	18	68	
14	197	85		57	318	84	11N
15	5	69	87N	58	293	48	47N
16	43	88		59	242	84	
17	286	54	74W	60	138	86	
18	36	80	72S	61	188	70	
19	279	78		62	236	86	
20	116	86		63	120	62	65N
21	191	73	36S	64	173	89	
22	25	83	81S	65	168	80	5N
23	202	83		66	164	76	5N
24	196	73		67	162	80	16N
25	334	89	68N	68	197	40	
26	357	49	67N	69	305	67	
27	193	58	61N	70	270	61	10S
28	171	39	86N	71	11	88	
29	157	88	81S	72	242	86	12N
30	212	58		73	238	87	
31	7	84		74	149	79	7N
32	357	80	12N	75	178	71	76N
33	211	79	86N	76	182	89	
34	328	65	73S	77	243	83	
35	153	87		78	185	78	30N
36	348	86		79	178	82	
37	8	88		80	192	85	10S
38	44	85	53N	81	179	66	
39	36	74	81N	82	351	64	14N
40	23	73	82N	83	105	42	
41	9	64	81N	84	210	55	
42	186	72		85	214	47	
43	195	64		86	239	81	

Note: RHR= right hand rule.

TABLE 10. FAULT PLANES WITH RAKES STRIKE-SLIP FAULTS

Fault	Strike	Dip (RHR)	Trend	Rake	T Trend	T Plunge	P Trend	P Plunge
1	192	85	193	10	238	3	147	11
2	150	79	329	7	105	3	14	13
3	203	70	206	9	68	7	161	21
4	162	75	341	4	26	13	117	8
5	171	80	350	5	35	11	126	4
6	168	81	345	16	32	18	301	5
7	213	85	32	14	347	6	78	13
8	348	89	348	21	301	15	35	14
9	237	86	56	12	102	11	11	6
10	36	80	41	28	86	12	350	27
11	203	77	21	10	67	16	157	2
12	132	61	307	10	351	27	87	13
13	197	87	16	14	331	8	62	12
14	242	86	61	12	107	11	16	6

Note: RHR= right hand rule.
Used for Figure 7.

TABLE 11. FAULT PLANES WITH RAKES NORMAL FAULTS

Fault	Strike	Dip (RHR)	Trend	Rake	T Trend	T Plunge	P Trend	P Plunge
1	178	69	319	59	286	20	54	59
2	192	46	316	41	119	2	24	72
3	144	60	262	57	245	14	20	71
4	9	61	81	60	92	16	301	72
5	51	61	123	60	134	16	343	72
6	27	67	107	67	114	22	304	68
7	298	56	329	37	359	2	266	56
8	296	55	359	52	15	9	252	74
9	178	71	305	67	279	25	67	62
10	9	64	79	63	92	19	298	70
11	27	67	107	67	114	22	304	68
12	293	48	329	33	174	5	273	59

Note: RHR= right hand rule
Used for Figure 7.

Appendix II

Rock Descriptions

Alluvium 1-4 (Quaternary)- Mapped through NAIP imagery, detailed unit descriptions are not distinguished. Unit thickness is not available.

Tgd- Granodiorite of Cactus Stock (Tertiary)- Moderate to dark reddish-brown on the weathered surface, white on the fresh surface. Granite contains 1-3 mm crystals of plagioclase, biotite, quartz, hornblende, pyrite, and chalcopyrite. Local greenschist metamorphism containing chlorite. Indurated, contains white skarns and sills, tabular geometry, intrusive contacts. K-Ar age 28 Ma (Lemmon et al., 1973). Unit thickness is not available.

Ths- Horn Silver Andesite (Tertiary)- Brownish-orange and brownish-red on the weathered surface, pale purple to greyish purple on the fresh surface. Mainly consists of porphyritic flow rocks but also contains tuffs in the central part of the range. 50% total phenocrysts, phenocryst assemblage: plagioclase>biotite>quartz>hornblende with trace augite and magnetite. Contains flow foliations, friable, slope forming. K-Ar ages of 34.1-30.8 Ma (Lemmon et al., 1973). Unit thickness is up to 600 m.

Thr- Conglomerate of High Rock Pass (Tertiary)- Contains two units of conglomerate mostly concentrated in the central part of the range. Facies one: boulder conglomerate consisting of ~99% local limestones with a very small amount of quartzites, contains no volcanic clasts, well-rounded, clast supported, beige light brown silt to sand matrix, outcrop is not well exposed, slope and hill forming, coarsening upward with ~1 m size

boulders at the top of unit. Facies two: pebble to cobble conglomerate with some boulders ~0.5 m in size, consists of ~80% local quartzites and ~20% local limestones, contains no volcanic clasts, quartzite clasts are sub-angular, limestone clasts are sub-rounded, clast supported, red silt to sandy matrix, poorly sorted. Unit thickness is up to 100 m.

TKbr- Tectonic Breccia (Tertiary)- Mounds of intermittently outcropping cobble to boulder breccia. Clasts within each individual mound are distinct to a single lithologic unit of localized quartzites. Unit thickness is not available.

Owr- Watson Ranch Quartzite (Ordovician)- White to very light grey on the weathered surface, very white on the fresh surface, pale yellowish orange weathering pattern. Very fine to fine-grained, sugary crystalline texture, indurated, thick bedding, slope and ledge forming. Unit thickness is 90 m.

Pogonip Group (Ordovician)

Ok- Kanosh Shale (Ordovician)- Pale to moderate greenish yellow on the weathered surface, pale to light olive on the fresh surface, orange and black weathering pattern. Very fine-grain silt to very fine sand, thin bedding, contains fossils, slope forming. Also contains the Pogonip Limestone. Medium light to medium grey on the weathered surface, medium grey to dark grey on the fresh surface. Very fine to fine-grained, contains calcite veins, micrite, indurated, thick bedding, slope forming, contains brachiopods and bivalves. Unit thickness is 150 m.

Ojw- Juab and Wah Wah Limestones (Ordovician)- Medium grey on the weathered surface and contains moderate to dark reddish brown silty layers on the weathered

surface, medium bluish grey on the fresh surface. Very fine to fine-grained, micrite, thin bedding, contains spiral shells, slope forming. Abundant silty beds very diagnostic, silty beds give the unit a yellow tinge. Unit thickness is 120 m.

Ohf- Fillmore Formation and House Limestone (Ordovician)- Light bluish grey with yellowish grey on the weathered surface, medium grey on the fresh surface. Fine to medium-grained, medium bedding, some beds highly laminated, no fossils observed, cliff forming. Yellowish brown silt outcrop characteristics. Unit thickness is 700 m. Full thickness not observed due to low-angle normal faults.

OCn- Notch Peak Formation (Ordovician and Cambrian)- Limestone and dolostone, white to pinkish grey on the weathered surface, white and yellowish grey streaks on the fresh surface, rounded boulder weathering pattern. Fine to medium-grained, sparry, bedding thickness variable and difficult to observe, no fossils observed, slope forming. Heavily jointed and faulted. Contains moderate reddish orange sandy grains and laminations as outcrop characteristics. Unit thickness is 500 m. Full thickness not observed due to low-angle normal faults.

Cosp- Steamboat Pass Shale (Cambrian)- Very poorly or not exposed at the surface. Thickness not observed due to low-angle normal faults. Unit thickness is 60 m.

Cob- Big Horse Limestone (Cambrian)- Contains two facies of limestone. Facies one: very pale orange with pale yellow orange fracture fill on the weathered surface, white on the fresh surface. Very coarse-grained, recrystallized calcite, sparry, variable bedding sizes, some fine silty laminations and lenses, no fossils observed, cliff forming. Facies two: light to medium grey on the weathered and fresh surfaces. Grain size varies, recrystallized

calcite, sparry, contains thin silt beds, contains trilobite fragments, algae, stromatolites, cliff forming. Unit thickness is 280 m.

Cpm- Prospect Mountain Quartzite (Cambrian)- Unit description separated into upper and lower units. Upper: light to pale brown on the weathered surface, mix between pale pink, pale red purple, greyish red purple, and very dusky purple on the fresh surfaces, brownish orange to black weathering pattern. Coarse-grained, crystalline, abundant cross-bedding, thick bedding, some grains up to 5 mm in size, very sharp edges when broken, slope and ledge forming. Lower: light to pale brown on the weathered surface, pinkish grey on the fresh surface. Texturally different than the upper, sandier then the upper, fine to coarse-grained, contains grains not crystals, also contains some pebble metaconglomerate beds, slope forming. Unit thickness is 1000 m.

Zm- Mutual Formation (Precambrian)- Quartzite, pale red to greyish red on the weathered surface, slightly lighter whitish on the fresh surface, very pink outcrop characteristics, elephant skin or raindrop weathering pattern. Coarse to very coarse-grained, sub-rounded grains, contains gain-supported pebble metaconglomerate beds, contains some phyllitic bedding but less green in color when compared to the Inkom Formation, abundant cross-bedding, thick bedding >1 m, slope and ledge forming. Unit thickness is 600 m.

Zi- Inkom Formation (Precambrian)- Quartzite, dusky brown to very dusky red on the weathered surface, mainly greyish red but can vary to moderate orange pink on the fresh surface, very dark black varnish weathering pattern. Medium to coarse-grained, sub-angular grains, contains some lithic fragments with variable minerals, crystalline but sand grains may be visible, thick bedding, slope and ledge forming. In the upper part of the

section contains bedding of thinly laminated phyllite slate light olive grey in color. Unit thickness is 170 m.

Zcc- Caddy Canyon Quartzite (Precambrian)- Pale reddish brown on the weathered surface, greyish red on the fresh surface, dark yellowish orange and some white grey weathering pattern. Very fine to fine-grained, crystalline, sugary texture, primarily quartz arenite, densely faulted and fractured, thick bedding, slope and ledge forming. In the northern part of the range the unit contains light to medium grey beds, matrix-supported metaconglomerate with pebble size grains. Unit thickness is 600 m. Full thickness not observed due to thrust faulting.

Blackrock Canyon Limestone (Precambrian)

Zbcu- Upper Member- Argillite, dark yellowish brown to moderate brown on the weathered surface, same color but slightly lighter on the fresh surface. Outcrop is not well exposed and is buried by detritus of the Caddy Canyon Quartzite. Thinly laminated bedding that is heavily deformed and tightly folded, fine-grained, slope forming. Unit thickness is 50 m.

Zbcd- Middle Limestone and/or Dolomite Member- greyish to dusky brown on the weathered surface, dusky brown on the fresh surface. Limestone with quartz cement, contains tightly folded argillite beds, not well exposed and mostly buried by detritus of the Caddy Canyon Quartzite, mainly dark pieces in float, slope and flat lying topography. Unit thickness is 50 m.

Zbcl- Lower Member- Quartzite and argillite, white to very light grey to black orange brown on the weathered surface, very light grey on the fresh surface,

weathering pattern may be black varnish like the Inkom Formation. Very fine to fine-grained, crystalline, sugary texture, argillaceous, crystals may look like the Caddy Canyon Quartzite but whiter in comparison, some cross-bedding, medium bedded quartzite, thin bedded argillite, heavily strike-slip faulted, slope forming. Unit thickness is 200 m.

Zp- Pocatello Formation (Precambrian)- Argillite and quartzite. Reddish brown on the weathered and fresh surfaces. Thin laminations, not well exposed and mostly buried by detritus of the Blackrock Canyon Limestone. Unit thickness is 300 m. Full thickness not observed due to thrust faulting.

Appendix III

(U-Th)/He Thermochronology

A total of eleven samples were collected (3-6 kg each) in the study area for thermochronology analysis. Samples were collected in an ~E-W transect in the northern San Francisco Mountains. The samples collected are all from quartzite units in the hanging wall of the Frisco thrust. Samples were collected with at least ~700 m spacing and according to Stockli (2005), normal to the strike of major faults in the area. The samples will be used for bedrock (U/Th)-He thermochronology to give timing data and exhumation history for the Frisco thrust sheet.

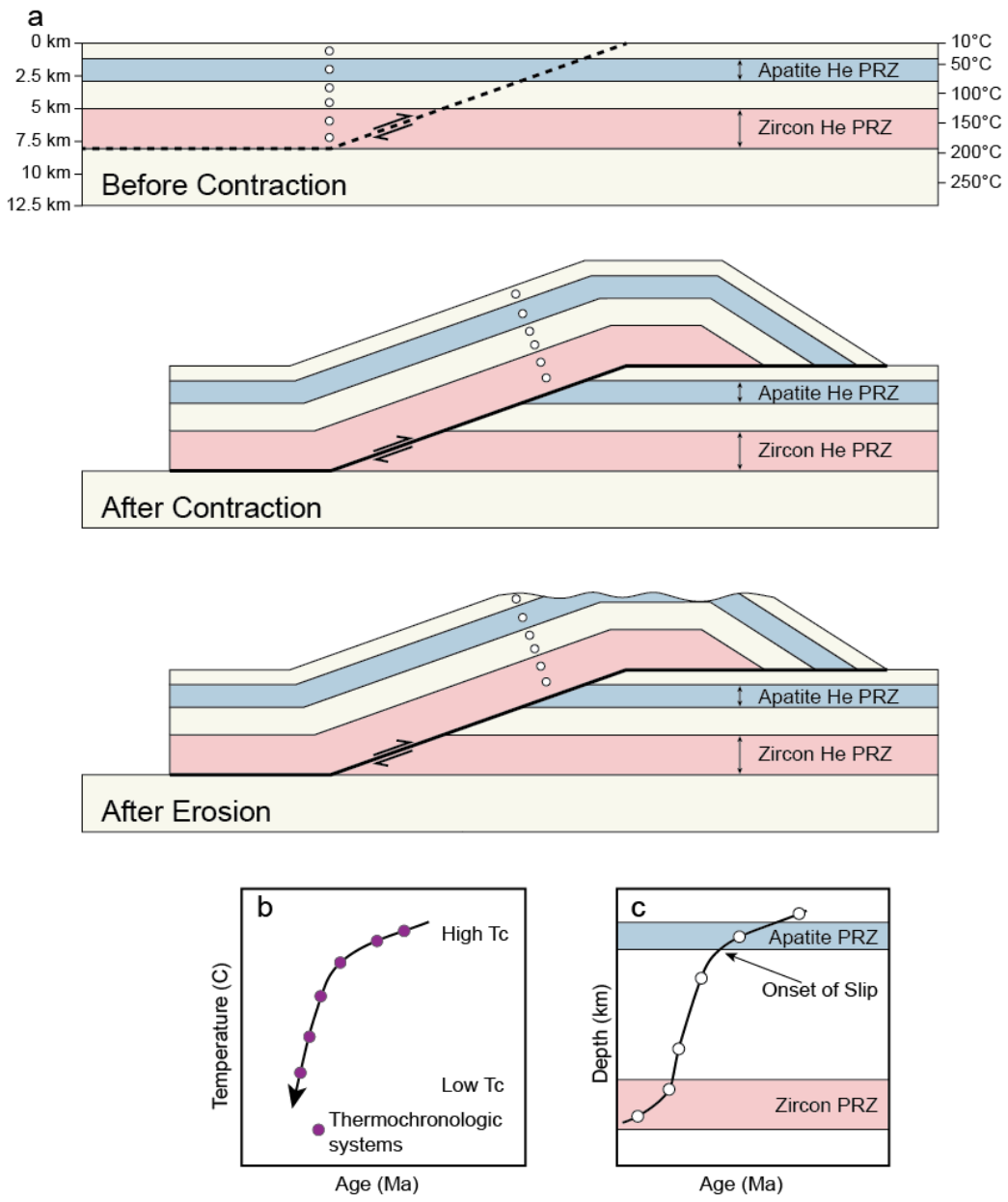

Figure 11. Thermochronology sampling strategy. (a) Schematic diagram showing three stages of thrust fault evolution for a single-ramp thrust. He PRZ's for apatite and zircon before and after thrusting with ideal sample collection from the hanging wall (circles). (b) Age-temperature and (c) age-depth plots to illustrate estimated timing of initiation of thrusting, cooling rate, exhumation rate. Modified from Eleogram (2014) and Stockli (2005).

TABLE 12. (U-TH)/HE THERMOCHRONOLOGY SAMPLES

Sample number	Unit name	Rock type	Longitude	Latitude	Elevation (m)
21SF01	Prospect Mountain Quartzite	Quartzite	-113.0340	38.7430	1587
21SF02	Prospect Mountain Quartzite	Quartzite	-113.0448	38.7463	1595
21SF03	Prospect Mountain Quartzite	Quartzite	-113.0986	38.7044	1730
21SF04	Prospect Mountain Quartzite	Quartzite	-113.0915	38.7098	1761
21SF05	Prospect Mountain Quartzite	Quartzite	-113.1045	38.6974	1591
21SF06	Mutual Formation	Quartzite	-113.1199	38.6955	1571
21SF07	Mutual Formation	Quartzite	-113.1299	38.6365	1662
21SF08	Inkom Formation	Quartzite	-113.1389	38.6416	1687
21SF09	Caddy Canyon Quartzite	Quartzite	-113.1589	38.6332	1915
21SF11	Mutual Formation	Quartzite	-113.2282	38.6333	1745
21SF12	Prospect Mountain Quartzite	Quartzite	-113.2339	38.6362	1704

References

Abbott, J.T., Best, M.G., and Morris, H.T., 1983, Geologic map of the Pine Grove-Blawn Mountain Area, Beaver County, Utah: Department of the Interior United States Geological Survey, scale 1:24,000, 2 sheets.

Allmendinger, R.W., 2019, FaultKin, v. 8.1.2, copyrighted software.

Allmendinger, R.W., 2021, Stereonet, v. 11.3.6, copyrighted software.

Allmendinger, R.W., and Jordan, T.E., 1981, Mesozoic evolution, hinterland of the Sevier orogenic belt: Geology, v. 9, p. 308-313.

Allmendinger, R. W., Cardozo, N., and Fisher, D., 2012, Structural geology algorithms: Vectors and tensors in structural geology: Cambridge University Press, p. 302.

Allmendinger, R. W., Cardozo, N. C., and Fisher, D., 2013, Structural Geology Algorithms: Vectors & Tensors: Cambridge, England, Cambridge University Press, 289 pp.

Anders, M.H., Christie-Blick, N., and Malinverno, A., 2012, Cominco American well: implications for the reconstruction of the Sevier orogen and Basin and Range extension in west-central Utah: American Journal of Science, v. 312, p. 508–533.

Best, M.G., Lemmon, D.M., and Morris, H.T., 1989, Geologic Map of the Milford Quadrangle and East Half of the Frisco Quadrangle, Beaver County, Utah: U.S. Geological Survey, scale 1:48,000, 1 sheet.

Burtner, R.L., and Nigrini, A., 1994, Thermochronology of the Idaho-Wyoming thrust belt during the Sevier orogeny; A new, calibrated, multiprocess thermal model: American Association of Petroleum Geologists Bulletin, v. 78, p. 1568-1612.

Canada, A.S., Cassel, E.J., Stockli, D.F., Smith, M.E., Jicha, B.R., and Singer, B.S., 2019, Accelerating exhumation in the Eocene North American Cordilleran hinterland: Implications from detrital zircon (U-Th)/(He-Pb) double dating: GSA Bulletin, doi:10.1130/b35160.1.

Cardozo, N., and Allmendinger, R. W., 2013, Spherical projections with OSXStereonet: Computers & Geosciences, v. 51, no. 0, p. 193 - 205, doi: 10.1016/j.cageo.2012.07.021.

Colgan, J.P., and Henry, C.D., 2009, Rapid middle Miocene collapse of the Mesozoic orogenic plateau in north-central Nevada: International Geology Review, doi:10.1080/00206810903056731.

Dahlstrom, C.D.A., 1969, Balanced Cross-sections: Canadian Journal of Earth Sciences,

v. 6, p. 743-757.

DeCelles, P.G., 2004, Late Jurassic to Eocene evolution of the Cordilleran thrust belt and foreland basin system, western U.S.A.: American Journal of Science, v. 304, p. 105-168.

DeCelles, P.G., and Coogan, J.C., 2006, Regional structure and kinematic history of the Sevier fold-and-thrust belt, central Utah: GSA Bulletin, v. 118, no. 7/8, p. 841-864, doi:10.1130/B25759.1.

Dickinson, W.R., 2006, Geotectonic evolution of the Great Basin: Geosphere, v. 2, no. 7, p. 353-368, doi:10.1130/GES00054.1.

Dover, J.H., 2007, Geologic map of the Logan 30' x 60' Quadrangle, Cache and Rich Counties, Utah and Lincoln and Uinta Counties, Wyoming: Utah Geological Survey, scale 1:100,000, 3 sheets.

Dunne, G.C., and Walker, J.D., 2004, Structure and Evolution of the East Sierran thrust system, east central California: Tectonics, v. 23, TC4012, doi:10.1029/2002TC001478.

East, E.H., 1965, Structure and Stratigraphy of the San Francisco Mountains, Western Utah: Bulletin of the American Association of Petroleum Geologists, v. 50, no. 5, p. 901-920.

Eleogram, Bryan, 2014, The Application of Zircon (U/Th)/He Thermochronology to Determine the Timing and Slip Rate on the Willard Thrust, Sevier Fold and Thrust Belt, Northern Utah: UNLV Theses, Dissertations, Professional Papers, and Capstones, 2078, http://dx.doi.org/10.34917/5836097.

Friedrich, A.M., and Bartley, J.M., 2003, Three-dimensional structural reconstruction of a thrust system overprinted by postorogenic extension, Wah Wah thrust zone, southwestern Utah: GSA Bulletin, v. 115, no. 12, p. 1473-1491.

Gibbs, A.D., 1983, Balanced cross-section construction from seismic sections in areas of extensional tectonics: Journal of Structural Geology, v. 5, no. 2, p. 153-160.

Groshong, R. H., Jr., 1994, Area balance, depth to detachment and strain in extension: Tectonics, v. 13, p. 1488-1497.

Gudmundsson, A., De Guidi, G., Scudero, S., 2013, Length-displacement scaling and fault growth: El Sevier, Tectonophysics 608, p. 1298-1309.

Hintze, L.F., and Davis, F.D., 2002, Geologic map of the Delta 30' x 60' Quadrangle and

part of the Lynndyl 30’ x 60’ Quadrangle, northeast Millard County and parts of Juab, Sanpete, and Sevier Counties, Utah: Utah Geological Survey, scale 1:100,000, 2 sheets.

Hintze, L.F., and Davis, F.D., 2002, Geologic map of the Wah Wah Mountains north 30’ x 60’ Quadrangle and part of the Garrison 30’ x 60’ Quadrangle, southwest Millard County and part of Beaver County, Utah: Utah Geological Survey, scale 1:100,000, 2 sheets.

Hintze, L.F., and Davis, F.D., 2003, Geology of Millard County, Utah: Utah Geological Survey a division of Utah Department of Natural Resources.

Hintze, L.F., Lemmon, D.M., and Morris, H.T., 1984, Geologic map of the Frisco Peak Quadrangle, Millard and Beaver Counties, Utah: U.S. Geological Survey, scale 1:48,000, 1 sheet.

Humphreys, E., 2009, Relation of flat subduction to magmatism and deformation in the western United States, Backbone of the Americas: Shallow Subduction, Plateau Uplift, and Ridge and Terrane Collision: Geological Society of America Memoir 204, p. 85–98, https:// doi .org /10 .1130 /2009 .1204 (04).

Ketcham, R.A., Donelick, R.A., Linn, J.K., and Walker, J.D., 1996, Effects of kinetic variation on interpretation and modeling of apatite fission track data; application to central Utah: Geological Society of America Abstracts with Programs, v. 28, no. 7, p. 441.

Lemmon, D.M., and Morris, H.T., 1984, Geologic map of the Beaver Lake Mountains Quadrangle, Millard and Beaver Counties, Utah: U.S. Geological Survey, scale 1:48,000, 1 sheet.

Lemmon, D.M., Silberman, M.L., and Kistler, R.W., 1973, Some K-Ar Ages of extrusive and intrusive rocks of the San Francisco and Wah Wah Mountains, Utah: Utah Geological Association.

Marrett, R. A., and Allmendinger, R. W., 1990, Kinematic analysis of fault-slip data: Journal of Structural Geology, v. 12, p. 973-986.

McQuarrie, N., and Wernicke, B.P., 2005, An animated tectonic reconstruction of southwestern North America since 36 Ma: Geosphere, v. 1, no. 3, p. 147-172; doi: 10.1130/GES00016.1.

Mitra, G., and Sussman, A.J., 1997, Structural evolution of connecting splay duplexes and their implications for critical taper: an example based on geometry and kinematics of the Canyon Range culmination, Sevier belt, central Utah: Journal of Structural Geology, v. 19, p. 506-521.

Miller, G.M., 1966, Structure and stratigraphy of southern part of Wah Wah Mountains, southwest Utah: Bulletin of the American Association of Petroleum Geologists, v. 50, no. 5, p. 858-900

Morris, H.T., 1983, Interrelations of thrust and transcurrent faults in the central Sevier orogenic belt near Leamington, Utah: Geological Society of America, memoir 157, p. 75-81.

Pujols, E.J., Stockli, D.F., Constenius, K.N., Horton, B.K., 2020, Thermochronological and geochronological constraints on late Cretaceous unroofing and proximal sedimentation in the Sevier Orogenic belt, Utah: Tectonics, v. 39, doi:10.1029/2019TC005794.

Rowan, M.G., and Kligfield, R., 1989, Cross-section restoration and balancing as aid to seismic interpretation in extensional terranes: The American Association of Petroleum Geologists Bulletin, v. 73, no. 8, p. 955-966.

Stockli, D.F., 2005, Application of Low-Temperature Thermochronometry to Extensional Settings: Reviews in Mineralogy & Geochemistry, v. 58, Mineralogical Society of America, p. 411-448.

Stockli, D.F., Linn, J.K., Walker, J.D., Dumitru, T.A., 2001, Miocene unroofing of the Canyon Range during extension along the Sevier Desert Detachment, west central Utah: Tectonics, v. 20, no. 3, p. 289-307.

Sussman, A.J., 1995, Geometry, deformation history and kinematics in the footwall of the Canyon Range thrust, central Utah: M.Sc. thesis, University of Rochester.

Sussman, A.J., and Mitra, G., 1995, Deformation patterns in the footwall of the Canyon Range thrust, central Utah: implications for Sevier fold-and-thrust belt development: Geological Society of America, Rocky Mountain Meeting Abstracts 27, 57.

U.S. Geological Survey, 2007, Preliminary integrated geologic map databases for the United States: http://pubs.usgs.gov/of/2005/1305/ (accessed January 2022).

Welsh, J.E., 1972, Upper Paleozoic stratigraphy plateau-Basin and Range transition zone central Utah: 2012 Utah Geological Association.

Wyld, S.J., and Wright, J.E., 2001, New evidence for Cretaceous strike-slip faulting in the United States Cordillera and implications for terrane-displacement, deformation patterns, and plutonism: American Journal of Science, v. 30, doi: https://doi.org/10.2475/ajs.301.2.150.

Yonkee, W.A., DeCelles, P.G., and Coogan, J.C., 1997, Kinematics and synorogenic

sedimentation of the eastern frontal part of the Sevier orogenic wedge, northern Utah, in Link, P.K., and Kowallis, B.J., eds., Proterozoic to recent stratigraphy, tectonics, and volcanology, Utah, Nevada, southern Idaho and central Mexico: Brigham Young University Geology Studies, v. 42, part 1, p. 355-380.

Yonkee, W.A., Eleogram, B., Wells, M.L., Stockli, D.F., Kelley, S., and Barber, D.E., 2019, Fault slip and exhumation history of the Willard thrust sheet, Sevier fold-thrust belt, Utah: Relations to wedge propagation, hinterland uplift, and foreland basin sedimentation: Tectonics, v. 38, doi:10.1029/2018TC005444.

Yonkee, W.A., Parry, W.T., Bruhn, R.L., and Cashman, P.C., 1989, Thermal models of thrust faulting: Constraints from fluid inclusion observations, Willard thrust sheet, Idaho-Utah-Wyoming thrust belt: Geological Society of America Bulletin, v. 101, p. 304-313.